Smiling twice: The Heston++ model

Smiling twice: The Heston++ model

Claudio Pacati[a,*], Gabriele Pompa[b], Roberto Renò[c]

[a] *Dipartimento di Economia Politica e Statistica, Università di Siena, Italy*
[b] *IMT School for Advanced Studies Lucca, Italy*
[c] *Dipartimento di Scienze Economiche, Università di Verona, Italy*

Abstract

We recommend the addition of a deterministic displacement to multi-factor affine models to calibrate and hedge SPX and VIX derivatives *jointly*. The proposed model, labeled Heston++, calibrates both markets with an average relative error (on quoted implied volatilities over two years of data) of 2%, and a *maximum* relative error of 4%, without additional computational costs with respect to traditional affine benchmarks. Hedging performance on both markets is also drastically improved. The displacement can be interpreted as a *volatility push-up* reflecting expectations about a (risk-neutral) lower bound on forward VIX dynamics. Our empirical results document substantial correlation between the dynamics of the displacement and the variance risk premium, and still provide strong support for the presence of both price/volatility negatively correlated co-jumps and idiosyncratic jumps in the volatility dynamics, even when the displacement is added.

Keywords: VIX options, VIX futures, Heston model, stochastic volatility, jump-diffusion, displacement
JEL: G12, G13

*Corresponding author. Dipartimento di Economia Politica e Statistica, Università di Siena, piazza S. Francesco, 7, 53100 Siena (Italy). Tel. +39 0577 232772, fax. +39 0577 232661.

Email addresses: claudio.pacati@unisi.it (Claudio Pacati), gabriele.pompa@imtlucca.it (Gabriele Pompa), roberto.reno@univr.it (Roberto Renò)

1. Introduction

The growing demand for trading volatility and managing volatility risk leaded to the creation of a liquid market for derivatives on realized variance. The Chicago Board Options Exchange (CBOE) introduced, in 1993, the VIX volatility index, also known as the *Fear Index*, and later on started trading derivatives written on it: VIX futures (in 2004) and VIX options (in 2006). The increased popularity of these assets has made volatility a commonly accepted asset class. Surprisingly, there has been very little effort in the literature to test pricing models on the two markets jointly. As we document in what follows, this mainly depends on the difficulty of traditional continuous-time affine models in providing a reasonable calibration of both markets.

The purpose of this paper is then to propose a simple addition to affine models which is able to calibrate the two "smiles" with a single set of parameters, without adding further computational complications. With respect to traditional models in continuous time, we add a new ingredient: a deterministic displacement in the spirit of Brigo and Mercurio (2001). While originally devised to improve the fitting of the term structure in interest rate models, we show that this device is also extremely useful for pricing and hedging stock index and variance derivatives. The new modeling framework, named Heston++, calibrates the prices of vanilla options written on the S&P 500 index (the first traditional "smile") consistently with VIX derivatives (futures and options, the second "smile"), with *maximum* estimation error of roughly 4% (relative to the market implied volatility), over a sample of more than 25,000 quoted prices. Moreover, it provides superior hedging performance with respect to non-displaced models: the hedging error (defined as the absolute value of the difference between the option and the replicating portfolio returns) is cut by roughly 25% for SPX options and by roughly 10% on VIX options for a static replication with basic instruments over one week. The displacement represents a lower bound to forward VIX dynamics, a desirable feature since historical VIX is far from zero. The displacement adds flexibility to the model, allowing a better matching of higher order moments (skewness and kurtosis), which are crucial for nonlinear payoffs. The empirical correlation between fitted displacements and the variance risk premium indicates that the displacement can be used by the aggregate trader not only as a "support variance" but, potentially, also as a "support risk premium" when pricing variance derivatives.

Even if theoretical approaches for VIX modeling are abundant in the literature, they are typically focused on just one of the two markets. They can be broadly divided in two categories: a *standalone* and a *consistent* approach. In the standalone approach, the volatility is modeled without specifying the dynamics of the underlying price. Earlier contributions to this field are Whaley (1993), who assumes VIX to follow a Geometric Brownian Motion, Grünbichler and Longstaff (1996) and Detemple and Osakwe (2000), who allow for mean-reversion, while Psychoyios et al. (2010) allow for jumps. Mencía and Sentana (2013) perform an extensive empirical analysis of several standalone specifications, providing empirical support for upward VIX jumps, time-varying central tendency and stochastic volatility of VIX. However, although closed-form expressions for VIX derivatives prices are readily obtainable in this framework, the tractability of this approach comes at expense of the inability to check the consistency with vanilla options. In the second research stream, consistent approaches specify a joint dynamics for the underlying and its volatility. Typically an affine model, such as the popular Heston (1993), is assumed for SPX dynamics (see, e.g., Zhang and Zhu, 2006, extended by Zhang et al., 2010 to allow for stochastic mean reversion). This framework can then be extended with jumps in volatility (Lin, 2007; Sepp, 2008a,b; Zhu and Lian, 2012; Lian and Zhu, 2013) and/or with multi-factor specifications (Chen and Poon, 2013; Lo et al., 2013). Bayer et al. (2013) adopted a double mean reverting CEV model to consistently price SPX and VIX options, Cont and Kokholm (2013) considered an affine Lévy specification, Chen and Poon (2013) multi-factor Heston specifications and finally Papanicolaou and Sircar (2014) added sharp volatility regime shifts to a Heston dynamics. Since the same volatility process underlies both equity and volatility derivatives, as shown in the

above mentioned contributions, this class of models can be used to price VIX derivatives as well. However, none of the above mentioned studies used the joint information of vanilla options and variance derivatives in empirical exercises. More recently, the two markets have been started to be analyzed jointly. Chung et al. (2011) use the information in both markets to forecast realized volatility; Song and Xiu (2016) use these two markets to estimate the dependence of the pricing kernel on the volatility factors; and Bardgett et al. (2018) estimate a dynamic model on both markets to gain resolution on the risk premia. Kokholm and Stisen (2015) also perform a joint calibration exercise, similar to that in this paper; they however analyze only few days obtaining results which are hard to be considered satisfactory.

Our model is consistent with the consistent approach, is an affine model, and is successfully applied to the joint calibration and hedging of both markets on a time span of two recent years. Formally, our model belongs to the class of affine models studied in Duffie et al. (2000). It could also be seen as a special case of Stochastic Local Volatility (SLV) models (see e.g. Tian et al., 2015 and the references therein), and in particular of a displaced diffusion. The model was first introduced explicitly by Pacati et al. (2014), where it was shown that the deterministic shift can dramatically improve the calibration of the term structure of at-the-money vanilla options, thus improving sensibly the fit of the whole vanilla surface. In this paper, after extending their model by adding jumps in volatility, we show that the displacement is extremely effective on variance derivatives as well, since it provides a handy lower bound for VIX futures. The class of models endowed with the deterministic shift extension is labeled Heston++, since it parallels the structure of the CIR++ model of Brigo and Mercurio (2001).

These two additions (displacement and jumps in volatility) are interconnected, since jumps in volatility are particularly well identified by the price of variance derivatives. We indeed not only show that the deterministic shift provides the necessary flexibility to calibrate the term structure of VIX futures and the surface of VIX options thoroughly, without compromising the excellent fit on vanilla options (two "smiles" at once), but we also exploit the additional information content provided by variance derivatives to learn about the features of the price dynamics. For example, we provide strong support for the contemporaneous presence of two kinds of jumps in volatility, the first being correlated with jumps in the index (typically, accounting for market downturns accompanied by a spike in volatility, as also empirically supported by Todorov and Tauchen, 2011 and Bandi and Renò, 2016), and the second being independent from price movements and accounting for spikes in volatility not accompanied by changes in the index. Our empirical findings suggest that both sources of risk are present in the data, and thus that both need to be hedged. In particular, idiosyncratic jumps in volatility appear to be particularly relevant for the pricing of VIX options, especially for the short term.

The paper is structured as follows. In Section 2 we specify the model adopted in our empirical investigations together with the closed-form pricing expressions for SPX vanilla options and VIX index and derivatives. In Section 3 we describe our calibration exercise. Section 4 is devoted to the hedging exercise and to the assessment of the out-of-sample performance of the model. In Section 5, we discuss the economic significance of the added displacement. Section 6 concludes. Appendix A collects technical results, while Appendix B provides details on the implementation.

2. Pricing VIX derivatives with the Heston++ model

In this section we introduce the Heston++ class of models for the dynamics of the underlying price. It is an affine class with a deterministic shift extension in the spirit of Brigo and Mercurio (2001). We then provide pricing formulas for equity and variance futures and options.

2.1. Model specification

We consider a filtered probability space $(\Omega, \mathcal{F}, \{\mathcal{F}_t\}_{t\geq 0}, \mathbb{Q})$, satisfying usual assumptions. Under the risk-neutral measure $\mathbb{Q}$, we specify the evolution of the logarithmic price of the underlying $x_t = \log S_t$ as follows

$$\begin{cases} dx_t = \left[r - q - \lambda\bar{\mu} - \frac{1}{2}\left(\sigma_{1,t}^2 + \phi_t + \sigma_{2,t}^2\right)\right]dt + \sqrt{\sigma_{1,t}^2 + \phi_t}\, dW_{1,t}^S + \sigma_{2,t} dW_{2,t}^S + c_x dN_t \\ d\sigma_{1,t}^2 = \alpha_1(\beta_1 - \sigma_{1,t}^2)dt + \Lambda_1\sigma_{1,t} dW_{1,t}^\sigma + c_\sigma dN_t + c'_\sigma dN'_t \\ d\sigma_{2,t}^2 = \alpha_2(\beta_2 - \sigma_{2,t}^2)dt + \Lambda_2\sigma_{2,t} dW_{2,t}^\sigma \end{cases} \tag{1}$$

where r is the short rate, q is the continuously compounded dividend yield rate, and in which the risk-neutral dynamics of the index is driven by continuous and discontinuous shocks, modeled by the Wiener processes $W_{i,t}^S, W_{i,t}^\sigma$ $(i = 1, 2)$ and the independent Poisson processes N_t, N'_t respectively. The short rate and the dividend rate are kept constant for simplicity, but could be easily made time-varying, for example as in Bakshi et al. (1997). The first volatility factor is *displaced*, as in Pacati et al. (2014), by a sufficiently regular deterministic function ϕ_t which verifies:

$$\phi_t \geq 0 \;\text{ and }\; \phi_0 = 0 \;\; . \tag{2}$$

Parameters $\alpha_i, \beta_i, \Lambda_i$ $(i = 1, 2)$ are non-negative constants. The effect of the displacement ϕ_t is to shift the (risk-neutral) integrated variance distribution upward. Indeed, it moves the lower bound of the instantaneous volatility of x_t from 0 (the affine case) to $\sqrt{\phi_t}$ (the displaced case). In terms of integrated volatility, that is in terms of VIX, this is equivalent to providing an additional deterministic term to the minimum attainable by the probability density function of the forward VIX, which is explicitly computed in Proposition 2. We denote this model with the generic label Heston++. The corresponding dynamics of the index S_t is, by Itō's lemma:

$$\frac{dS_t}{S_{t-}} = (r - q - \lambda\bar{\mu})\, dt + \sqrt{\sigma_{1,t}^2 + \phi_t} dW_{1,t}^S + \sigma_{2,t} dW_{2,t}^S + (e^{c_x} - 1)\, dN_t \;\; . \tag{3}$$

All correlations among Wiener processes are zero, with the exception of the following ones, which are defined as

$$\begin{aligned} \operatorname{corr}(dW_{1,t}^S, dW_{1,t}^\sigma) &= \rho_1 \sqrt{\frac{\sigma_{1,t}^2}{\sigma_{1,t}^2 + \phi_t}} \;\; , \\ \operatorname{corr}(dW_{2,t}^S, dW_{2,t}^\sigma) &= \rho_2 \;\; , \end{aligned}$$

where $\rho_1, \rho_2 \in [-1, 1]$ are constants. This choice guarantees that the model is affine according to the specification analysis of Dai and Singleton (2002), see also Collin-Dufresne et al. (2008) and Cheridito et al. (2010).

The Poisson processes N_t and N'_t are independent and also independent from all the Wiener processes. Their intensities are given by the constant parameters λ and λ' respectively. They drive jumps in price and jumps in volatility. The first Poisson process N_t is responsible for correlated jumps, occurring simultaneously in price and volatility, with sizes c_x and c_σ respectively. The second Poisson process N'_t is instead responsible for idiosyncratic jumps in volatility, with size c'_σ, independent from all other shocks. Jumps in volatility are exponentially distributed, with parameters $\mu_{co,\sigma}$ and $\mu_{id,\sigma}$ expressing the mean of correlated and idiosyncratic jumps respectively. Jumps in price are conditionally (to jumps in volatility) normally distributed with

conditional mean $\mu_x + \rho_J c_\sigma$ and variance δ_x^2. The characteristic functions of the jump sizes are thus given by:

$$\begin{aligned} \theta^{co}(z_x, z_\sigma) &= \mathrm{E}^{\mathbb{Q}}\left[e^{ic_x z_x + ic_\sigma z_\sigma}\right] = \frac{e^{i\mu_x z_x - \frac{1}{2}\delta_x^2 z_x^2}}{1 - i\mu_{co,\sigma}\left(z_\sigma + \rho_J z_x\right)} \ , \\ \theta^{id}(z'_\sigma) &= \mathrm{E}^{\mathbb{Q}}\left[e^{ic'_\sigma z'_\sigma}\right] = \frac{1}{1 - i\mu_{id,\sigma} z'_\sigma} \ , \end{aligned} \tag{4}$$

where $z_x, z_\sigma, z'_\sigma \in \mathbb{C}$.[1] We define $\bar{\mu} = \mathrm{E}^{\mathbb{Q}}\left[e^{c_x} - 1\right] = \theta^{co}(-i, 0) - 1$, so that the price jump compensator is $\lambda\bar{\mu}t$.

The Heston++ model (1) belongs to the affine class of Duffie et al. (2000). In case of no displacement ($\phi_t \equiv 0$), the model nests several models already analyzed in the literature:

- Imposing $\sigma_{2,t} \equiv 0$, several one-factor specifications can be obtained:
  - The standard SV model of Heston (1993) if $N_t \equiv N'_t \equiv 0$ is additionally imposed.
  - If $N'_t \equiv z_\sigma \equiv 0$ (i.e. allowing for log-normal jumps in price only) we have the SVJ, which is considered for example in Bates (1996) and Bakshi et al. (1997).
  - The SVCJ model, extensively studied in the equity pricing literature (see Eraker et al., 2003, Eraker, 2004 and Broadie et al., 2007 among others), is obtained by switching off the N'_t Poisson process and imposing $\sigma_{2,t} \equiv 0$. This model is considered for the pricing of futures and options on VIX by Lin (2007), Zhu and Lian (2012), Lian and Zhu (2013) and Kokholm and Stisen (2015).
  - If $N_t \equiv \sigma_{2,t} \equiv 0$, we obtain the SVVJ model which features idiosyncratic jumps in volatility. The SVVJ model is adopted by Sepp (2008b) for VIX option pricing extended with a local volatility term.

- Two-factor specifications can be obtained letting $\sigma_{2,t} > 0$:
  - The double Heston 2-SV model of Christoffersen et al. (2009) is obtained imposing no jumps $N_t \equiv N'_t \equiv 0$.
  - If $N'_t \equiv z_\sigma \equiv 0$, the 2-SVJ of Bates (2000) with constant jump intensity is obtained. A displaced version of this model, which we label 2-SVJ++, was considered in Pacati et al. (2014).
  - Finally if $N'_t \equiv 0$ we obtain the 2-SVCJ model considered by Lo et al. (2013) and Chen and Poon (2013) for VIX derivatives pricing.

The corresponding displaced models are obtained letting $\phi_t \geq 0$ and are labeled as their $\phi_t \equiv 0$ counterparts, with the suffix ++. Without restrictions, we label the model by 2-SVCVJ. The unrestricted model has in total 17 parameters plus the function ϕ_t. Two-factor model taxonomy is summarized in Table 1. Since this paper is interested in determining the empirical properties of the displacement with respect to non-displaced models, in what follows we focus only on the "largest" 2-SVCVJ and 2-SVCVJ++ models which, with a slight abuse of terminology, will be referred to as the Heston and the Heston++ model, or just as $\mathcal{H}$ and $\mathcal{H}$++ models (referring also to their nested specifications).

2.2. SPX and VIX derivatives pricing

The analytical tractability of the displaced models $\mathcal{H}$++ directly stems from the properties of non-displaced specifications $\mathcal{H}$. The following Lemma summarizes the relation among the log-price and volatility characteristic functions of the $\mathcal{H}$ and $\mathcal{H}$++ models. All proofs and mathematical details are contained in Appendix A.

[1] Jumps characteristic functions in equation (4) can be extended to the complex plane as long as $\mathrm{Im}(z_\sigma + \rho_J z_x) > -1/\mu_{co,\sigma}$ and $\mathrm{Im}(z'_\sigma) > -1/\mu_{id,\sigma}$, respectively. This implies the parameter restriction $\rho_J < 1/\mu_{co,\sigma}$ which is assumed throughout the present analysis and which is often satisfied by market calibrated correlation parameter, as it is usually found $\rho_J \leq 0$.

Table 1: Taxonomy of two-factor models.

model	jumps in			displacement
	price	volatility		
		idiosyncratic	co-jumps	
2-SV				
2-SV++				✓
2-SVJ	✓			
2-SVJ++	✓			✓
2-SVCJ	✓		✓	
2-SVCJ++	✓		✓	✓
2-SVVJ	✓	✓		
2-SVVJ++	✓	✓		✓
2-SVCVJ	✓	✓	✓	
2-SVCVJ++	✓	✓	✓	✓

Lemma 1. *Under the $\mathcal{H}$++ models, the time t conditional characteristic function of time $T > t$ returns $f_x^{\mathcal{H}++}(z) = \mathrm{E}^{\mathbb{Q}}\left[e^{izx_T} \,\middle|\, \mathcal{F}_t\right]$, and of the two stochastic volatility factors $f_\sigma^{\mathcal{H}++}(z_1, z_2) = \mathrm{E}^{\mathbb{Q}}\left[e^{iz_1\sigma_{1,T}^2 + iz_2\sigma_{2,T}^2} \,\middle|\, \mathcal{F}_t\right]$ are given by:*

$$\begin{aligned} f_x^{\mathcal{H}++}(z; x_t, \sigma_{1,t}^2, \sigma_{2,t}^2, t, T, \phi) &= f_x^{\mathcal{H}}(z; x_t, \sigma_{1,t}^2, \sigma_{2,t}^2, \tau) e^{-\frac{1}{2}z(i+z)I_\phi(t,T)} \ , \\ f_\sigma^{\mathcal{H}++}(z_1, z_2; \sigma_{1,t}^2, \sigma_{2,t}^2, \tau) &= f_\sigma^{\mathcal{H}}(z_1, z_2; \sigma_{1,t}^2, \sigma_{2,t}^2, \tau) \ , \end{aligned} \tag{5}$$

where $\tau = T - t$, $z, z_1, z_2 \in \mathbb{C}$ and $I_\phi(t,T) = \int_t^T \phi_s ds$.

Lemma 1 implies closed-form pricing formulas for vanilla options and variance derivatives for all the $\mathcal{H}$++ models by a modification of the conditional characteristic functions under the corresponding $\mathcal{H}$ model. For both classes of derivatives, we borrow from the results of Lewis (2000, 2001), which turn out to be convenient for numerical implementation.

Proposition 1. *Under the $\mathcal{H}$++ models, the arbitrage-free price at time t of a European call option on the underlying S_t, with strike price K and time to maturity $\tau = T - t$, is given by*

$$C_{\mathrm{SPX}}^{\mathcal{H}++}(K,t,T) = S_t e^{-q\tau} - \frac{1}{\pi}\sqrt{S_t K} e^{-\frac{1}{2}(r+q)\tau} \int_0^\infty \mathrm{Re}\left[e^{iuk - i\left(u-\frac{i}{2}\right)[x_t - y_t + (r-q)\tau]} f_x^{\mathcal{H}}\left(u - \frac{i}{2}\right)\right] \frac{e^{-\left(u^2+\frac{1}{4}\right)I_\phi(t,T)}}{u^2 + \frac{1}{4}} du \ , \tag{6}$$

where $k = \log\left(\frac{S_t}{K}\right) + (r-q)\tau$ and y is the exponential martingale such that $S_t = S_0 e^{(r-q)t + y_t}$.

The price dynamics under the $\mathcal{H}$++ models also determines the dynamics of the volatility index. In practice, the VIX quotation at time t is computed by CBOE as a model-free replication of the risk-neutral integrated variance over the following 30 days, using a portfolio of out-of-the-money options on S&P500 over a discrete grid of strike prices. In the present analysis, we instead adopt a standard definition for the variance index, expressed as the risk-neutral expectation of a log-contract (Jiang and Tian, 2005; Lin, 2007; Duan and Yeh, 2010; Zhang et al., 2010):

$$\left(\frac{\mathrm{VIX}_{t,\bar\tau}}{100}\right)^2 := -\frac{2}{\bar\tau}\mathrm{E}^{\mathbb{Q}}\left[\log\left(\frac{S_{t+\bar\tau}}{F_{t,t+\bar\tau}}\right)\middle|\, \mathcal{F}_t\right] \ , \tag{7}$$

where $F_{t,t+\bar\tau} = e^{(r-q)\bar\tau} S_t$ denotes the forward index quotation. For the CBOE VIX, $\bar\tau = 30$ days. The following Proposition gives the expression of $\mathrm{VIX}_{t,\bar\tau}$ under the $\mathcal{H}$ models and the effect of the displacement ϕ_t on the index dynamics.

Proposition 2. *Under the $\mathcal{H}$++ models,*

$$\left(\frac{\mathrm{VIX}^{\mathcal{H}++}_{t,\bar{\tau}}}{100}\right)^2 = \left(\frac{\mathrm{VIX}^{\mathcal{H}}_{t,\bar{\tau}}}{100}\right)^2 + \frac{1}{\bar{\tau}} I_\phi(t, t+\bar{\tau}) \ , \tag{8}$$

where $(\mathrm{VIX}^{\mathcal{H}}_{t,\bar{\tau}}/100)^2$ *is the corresponding quotation under* $\mathcal{H}$ *models, which is an affine function of the volatility factors* $\sigma^2_{1,t}$ *and* $\sigma^2_{2,t}$

$$\left(\frac{\mathrm{VIX}^{\mathcal{H}}_{t,\bar{\tau}}}{100}\right)^2 = \frac{1}{\bar{\tau}}\left(\sum_{k=1,2} a_k(\bar{\tau})\sigma^2_{k,t} + b_k(\bar{\tau})\right) \ , \tag{9}$$

where $I_\phi(t, t+\bar{\tau}) = \int_t^{t+\bar{\tau}} \phi_s ds$*; the exact forms of* $a_k(\bar{\tau})$ *and* $b_k(\bar{\tau})$ *are provided in Appendix A.*

Pricing of VIX derivatives is complicated by the non-affinity of VIX with respect to the volatility process. The arbitrage-free price $F_{\mathrm{VIX}}(t,T)$ at time t of a futures contract in VIX with maturity T cannot be derived as a simple cost-of-carry relationship, see Zhang et al. (2010) for an extensive discussion. It has to be evaluated as the risk neutral expectation of the VIX at settlement, see also Bardgett et al. (2018) and the discussion therein. Call options on VIX with maturity T and strike K are European-style options paying the amount $(\mathrm{VIX}_T - K)^+$ at maturity. They satisfy the put-call parity relation (Lian and Zhu, 2013) and no arbitrage conditions (Lin and Chang, 2009) with respect to VIX futures price, and their implied volatility can be inverted with the Black-76 formula (Papanicolaou and Sircar, 2014). They can be regarded as options on VIX futures, and can be priced according to standard risk-neutral evaluation $C_{\mathrm{VIX}}(K,t,T) = e^{-r\tau}\,\mathrm{E}^{\mathbb{Q}}\left[(\mathrm{VIX}_T - K)^+ \,\middle|\, \mathcal{F}_t\right]$. We solve the complications related to the non-linear relation between VIX and volatility by taking advantage of the analytical tractability of the conditional characteristic function of the volatility factors $f^{\mathcal{H}++}_\sigma(z_1, z_2)$ in Lemma 1, and of the generalized Fourier transform techniques of Lewis (2000, 2001) and Chen and Joslin (2012). We provide an explicit pricing formula for futures and options on VIX for $\mathcal{H}$++ models in the following Proposition. Similar results can be found in Sepp (2008a), Sepp (2008b), Lian and Zhu (2013) and Branger et al. (2014).

Proposition 3. *Under* $\mathcal{H}$++ *models, the time* t *value of a futures on* $\mathrm{VIX}_{t,\bar{\tau}}$ *settled at time* T *and the arbitrage-free price at time* t *of a call option on* $\mathrm{VIX}_{t,\bar{\tau}}$*, with strike price* K *and time to maturity* $\tau = T - t$ *are given respectively by*

$$F^{\mathcal{H}++}_{\mathrm{VIX}}(t,T) = 100 \times \frac{1}{2\sqrt{\pi}} \int_0^\infty \mathrm{Re}\left[f^{\mathcal{H}}_\sigma\left(-z\frac{a_1(\bar{\tau})}{\bar{\tau}}, -z\frac{a_2(\bar{\tau})}{\bar{\tau}}\right) \frac{e^{-iz\left(\sum_{k=1,2} b_k(\bar{\tau}) + I_\phi(T,T+\bar{\tau})\right)/\bar{\tau}}}{(-iz)^{3/2}} \right] d\,\mathrm{Re}(z) \ , \tag{10}$$

and

$$\begin{aligned} C^{\mathcal{H}++}_{\mathrm{VIX}}(K,t,T) = 100 \times \frac{e^{-r\tau}}{2\sqrt{\pi}} \int_0^\infty \mathrm{Re}\Bigg[& f^{\mathcal{H}}_\sigma\left(-z\frac{a_1(\bar{\tau})}{\bar{\tau}}, -z\frac{a_2(\bar{\tau})}{\bar{\tau}}\right) \\ & \times \frac{e^{-iz\left(\sum_{k=1,2} b_k(\bar{\tau}) + I_\phi(T,T+\bar{\tau})\right)/\bar{\tau}} \left(1 - \mathrm{erf}(K/100\sqrt{-iz})\right)}{(-iz)^{3/2}} \Bigg] d\,\mathrm{Re}(z) \ , \end{aligned} \tag{11}$$

where $z = \mathrm{Re}(z) + i\,\mathrm{Im}(z) \in \mathbb{C}$*,* $0 < \mathrm{Im}(z) < \zeta_c(\tau)$*,* $\zeta_c(\tau)$ *is given in Appendix A, and* $\mathrm{erf}(z) = \frac{2}{\sqrt{\pi}} \int_0^z e^{-s^2} ds$ *is the error function with complex argument.*

In this paper, we do not assume any explicit functional form for the displacement function ϕ_t. Once the set of derivatives on which the model has to be calibrated is fixed, with its finite set of maturities, an inspection of the pricing formulae shows that they depend only on the (finite number of) integrals of the displacement from each maturity to the next. We therefore calibrate all such integrals, denoted by I_ϕ; of course, this allows the immediate reconstruction of the integral of the displacement between any to maturities of the relevant set. The output of this calibration procedure is consistent with any functional form of the displacement having the same integrals, e.g. piecewise constant, piecewise linear, splines or other interpolation or functional methods. A detailed example of the displacement calibration is presented in Appendix B.1.

3. Pricing performance

Our sample period spans two years, 2009 and 2010. The sampling frequency used for calibration is weekly and the observation day is Wednesday. In total, we calibrate the Heston ($\mathcal{H}$) and the Heston++ ($\mathcal{H}$++) on 104 joint (SPX and VIX) surfaces and VIX Futures term-structures.

Commonly adopted exclusion filters are applied to data, see, e.g. Aït-Sahalia and Lo (1998) and Bakshi et al. (1997). We exclude option quotes with negative bid-ask spreads, zero bids and filter out observations not satisfying standard no-arbitrage conditions. Potential liquidity and asynchronicity biases are reduced by considering only options with maturity between one week and one year and excluding quoted contracts that are not traded on a given date. Following Bardgett et al. (2018), the analysis is carried out only with liquid out-of-the-money (OTM) options for the S&P500 market and only with liquid call options for the VIX market. If a VIX in-the-money (ITM) call is illiquid, we use the put-call parity to infer the liquid price of the call from a more liquid VIX OTM put (Lin and Chang, 2009).[2] We finally excluded three glaring outliers in the VIX option markets. The final sample is made of a total of 24,279 vanilla options (233 per day, on average), 2,767 VIX options (27 per day, on average), and 792 VIX futures (8 per day, on average). OTM vanilla (VIX call options) span on average 7 (5) maturity slices, ranging from 1 (4) weeks-to-maturity to 12 (6) months and from 0.5 (0.4) to 1.4 (3.3) in the moneyness dimension. The term structure of VIX futures ranges from roughly 7 days to 10 months. Vanilla option maturities range from one week to one year; VIX option maturities range from 4 weeks to 6 months. Summary statistics for S&P500 index options are presented in Table 2 and sample characteristics of VIX derivatives are presented in Table 3.

For each day in sample, we jointly calibrate the $\mathcal{H}$ and $\mathcal{H}$++ models to SPX and VIX option and futures market surfaces (the two "smiles"). Joint calibration is performed minimizing for each date in the sample the following loss function, representing the weighted sum of squared relative errors,

$$L = \frac{1}{N_{\text{SPX}}} \sum_{i=1}^{N_{\text{SPX}}} \left(\frac{\text{IV}^{\text{MKT}}_{i,\text{SPX}} - \text{IV}^{\text{mdl}}_{i,\text{SPX}}}{\text{IV}^{\text{MKT}}_{i,\text{SPX}}} \right)^2 + \frac{1}{N_{\text{Fut}}} \sum_{j=1}^{N_{\text{Fut}}} \left(\frac{F^{\text{MKT}}_j - F^{\text{mdl}}_j}{F^{\text{MKT}}_j} \right)^2 + \frac{1}{N_{\text{VIX}}} \sum_{k=1}^{N_{\text{VIX}}} \left(\frac{\text{IV}^{\text{MKT}}_{k,\text{VIX}} - \text{IV}^{\text{mdl}}_{k,\text{VIX}}}{\text{IV}^{\text{MKT}}_{k,\text{VIX}}} \right)^2 , \quad (12)$$

where N_{SPX} (N_{VIX}) are the number of S&P500 (VIX) options quotes observed, IV^{MKT} (IV^{mdl}) the corresponding market (model) implied volatilities and F^{MKT} (F^{mdl}) the market (model) VIX futures prices term structure, made of N_{Fut} points. The use of relative errors is suggested by the different range of implied volatility values of SPX and VIX options and normalizing factors $1/N_{\text{SPX}}$, $1/N_{\text{VIX}}$ and $1/N_{\text{Fut}}$ adjust for the difference in the number of quotes, which would otherwise penalize the fit of the term structure of VIX futures. Details on the calibration procedure can be found in Appendix B.1. We compare the pricing

[2] We consider as *liquid* a contract, either option or futures, which has both positive Volume and Open Interests.

Table 2: Sample characteristics of **SPX options**. The table reports the average prices, bid-ask spreads (BA), Black and Scholes (1973) implied volatilities (IV), bid-ask implied volatility spreads (IV BA), trading volume, open interests (OI), the total number of (and in percentage of the total) observations (Obs) for each moneyness-maturity category of call (Panel A) and put (Panel B) options on S&P500 index. The sample period is from January 7, 2009 to December 29, 2010 and the sampling frequency is weekly (Wednesdays). *Maturity* is defined as the number of days to expiration. *Moneyness* is defined as the ratio of the option exercise price to the current index level. ITM (OTM), ATM and OTM (ITM) for calls (puts) are defined by *Moneyness* < 0.95, $0.95 - 1.05$, and > 1.05, respectively.

Maturity	**Moneyness**							
	Panel A: Calls				**Panel B**: Puts			
	ITM	ATM	OTM	**All**	OTM	ATM	ITM	**All**
< 45 Days								
Price	90.84	24.61	2.02	30.12	2.99	24.54	81.08	15.77
BA	2.83	1.81	0.59	1.64	0.72	1.90	2.93	1.27
IV	30.43	22.92	20.14	23.48	36.35	23.39	20.19	30.92
IV BA	7.37	2.17	1.91	3.04	2.90	2.32	7.40	3.04
Volume	351.36	3,378.77	2,445.77	2,557.84	2,300.30	3,394.44	108.86	2,498.61
OI	19,734.07	25,392.34	17,186.77	21,987.46	23,523.10	22,979.02	9,930.25	22,350.05
Obs	863	2,507	1,373	4,743	4,232	2,316	517	7,065
Obs (% of TOT)	6.63	19.26	10.55	36.43	22.35	12.23	2.73	37.32
45 – 90 Days								
Price	114.58	36.67	5.64	29.27	8.51	39.45	112.74	21.76
BA	2.91	2.32	1.09	1.79	1.28	2.44	3.08	1.68
IV	30.37	23.97	19.93	22.65	35.79	24.78	21.21	32.13
IV BA	2.99	1.47	1.65	1.70	2.31	1.53	3.86	2.17
Volume	279.63	1,914.14	923.79	1,282.75	1,314.92	2,479.65	215.41	1,577.75
OI	20,349.71	16,199.80	10,566.55	13,897.48	18,797.49	17,432.34	11,966.58	18,107.94
Obs	459	2,034	2,295	4,788	4,710	1,862	324	6,896
Obs (% of TOT)	3.53	15.62	17.63	36.78	24.88	9.83	1.71	36.42
> 90 Days								
Price	149.66	64.52	17.69	48.92	24.24	71.85	168.24	46.99
BA	3.45	3.06	1.96	2.51	2.10	3.11	3.48	2.45
IV	30.20	25.35	21.16	23.64	34.77	25.90	22.24	31.67
IV BA	1.69	1.13	1.23	1.25	1.56	1.16	2.25	1.52
Volume	264.54	1,313.80	884.30	959.23	1,270.31	1,794.78	457.17	1,330.29
OI	23,226.76	24,169.13	24,861.13	24,436.20	32,406.18	22,356.63	20,350.24	2,9061.33
Obs	403	1,190	1,895	3,488	3,396	1,181	395	4,972
Obs (% of TOT)	3.10	9.14	14.56	26.79	17.94	6.24	2.09	26.26
All								
Price	110.90	37.18	8.85	34.84	10.95	40.15	117.23	26.15
BA spread	3.00	2.25	1.27	1.93	1.31	2.36	3.14	1.73
IV	30.36	23.80	20.40	23.22	35.70	24.43	21.12	31.56
IV BA spread	4.88	1.70	1.57	2.07	2.31	1.79	4.82	2.32
Volume	311.99	2,430.18	1,285.98	1,660.61	1,640.63	2,724.07	248.10	1,856.39
OI	20,713.86	21,875.81	17,069.84	19,668.26	24,164.15	20,914.65	13,794.06	22,567.39
Obs	1,725	5,731	5,563	13,019	12,338	5,359	1,236	18,933
Obs (% of TOT)	13.25	44.02	42.73	100.00	65.17	28.31	6.53	100.00

Table 3: Sample characteristics of **VIX futures and options**. The table reports the average prices, bid-ask spreads (BA), Black (1976) implied volatilities (IV), bid-ask implied volatility spreads (IV BA), trading volume, open interests (OI), the total number of (and in percentage of the total) observations (Obs) for each moneyness-maturity category of call (Panel A) and put (Panel C) options on VIX index. Panel B reports VIX futures settle prices, trading volume, open interests and observations for each maturity bucket. The sample period is from January 7, 2009 to December 29, 2010 and the sampling frequency is weekly (Wednesdays). *Maturity* is defined as the number of days to expiration. *Moneyness* for an option of maturity T is defined as the ratio of the option exercise price to the current VIX futures price expiring at T. ITM (OTM), ATM and OTM (ITM) for calls (puts) are defined by *Moneyness* < 1.0, $1.0 - 1.4$, and > 1.4, respectively.

Maturity	**Moneyness**								
	Panel A: Calls				**Panel B**: Futures	**Panel C**: Puts			
	ITM	ATM	OTM	**All**		OTM	ATM	ITM	**All**
< 45 Days									
Price	5.82	1.28	0.31	2.57	28.24	0.89	5.37	21.48	4.80
BA	0.32	0.13	0.11	0.19		0.12	0.29	0.53	0.24
IV	90.70	95.36	119.34	101.75		75.60	94.27	123.94	88.68
IV BA	32.40	6.16	12.12	17.48		7.58	15.17	51.35	14.97
Volume	1,316.87	4,842.85	2,848.60	2,920.52	5,008.29	6,821.95	1,620.99	27.74	3,750.20
OI	14,995.01	45,508.84	48,503.80	35,671.48	24,226.57	48,195.48	36,968.28	1,052.05	38,778.74
Obs	253	220	239	712	144	193	212	38	443
Obs (%)	8.08	7.03	7.63	22.74	18.18	12.89	14.16	2.54	29.59
45 – 90 Days									
Price	6.32	2.09	0.50	2.76	29.71	1.33	6.33	22.34	4.59
BA	0.37	0.19	0.14	0.23		0.16	0.32	0.51	0.24
IV	67.03	77.12	91.36	79.82		64.55	76.09	90.02	70.15
IV BA	13.52	4.13	7.79	8.58		5.35	7.12	26.09	7.62
Volume	852.46	2,382.41	1,038.02	1,349.91	1,698.15	1,723.83	678.05	19.54	1,266.86
OI	10,151.59	24,448.87	15,907.49	16,455.37	11,052.12	23,943.07	11,887.39	304.24	1,8340.82
Obs	239	210	314	763	144	250	122	34	406
Obs (%)	7.63	6.71	10.03	24.37	18.18	16.70	8.15	2.27	27.12
> 90 Days									
Price	7.12	2.73	0.84	3.70	29.99	1.71	6.90	19.30	3.61
BA	0.51	0.32	0.23	0.36		0.26	0.46	0.59	0.32
IV	55.77	63.56	73.84	63.96		55.84	63.11	74.08	58.26
IV BA	12.72	4.72	6.45	8.09		5.73	6.68	16.15	6.36
Volume	189.52	448.47	399.13	341.49	279.97	617.08	276.10	10.31	513.16
OI	28,27.80	4,751.16	3,674.41	3,737.78	2,629.10	5,930.87	2,583.38	166.52	4,918.10
Obs	587	559	510	1,656	504	470	153	25	648
Obs (%)	18.75	17.85	16.29	52.89	63.64	31.40	10.22	1.67	43.29
All									
Price	6.64	2.27	0.62	3.22	29.62	1.43	6.09	21.22	4.23
BA spread	0.44	0.25	0.17	0.29		0.21	0.35	0.54	0.27
IV	66.46	73.51	89.25	76.42		62.40	79.93	99.20	70.49
IV BA spread	17.51	4.91	8.12	10.34		6.02	10.49	33.42	9.25
Volume	600.70	1,836.63	1,138.58	1,173.71	1,397.51	2,231.79	962.25	20.37	1,675.49
OI	7,302.96	18,000.11	17,367.18	14,098.79	8,087.37	19,797.38	19,882.53	561.70	18,578.68
Obs	1,079	989	1,063	3,131	792	913	487	97	1,497
Obs (%)	34.46	31.59	33.95	100.00	100.00	60.99	32.53	6.48	100.00

performance of each model separately on each market in terms of the absolute errors

$$\mathrm{RMSE}_{\mathcal{M}} = \sqrt{\frac{1}{N_{\mathcal{M}}}\sum_{i=1}^{N_{\mathcal{M}}}\left(Q_{i,\mathcal{M}}^{\mathrm{MKT}} - Q_{i,\mathcal{M}}^{\mathrm{mdl}}\right)^2}\ , \tag{13}$$

and relative errors

$$\mathrm{RMSRE}_{\mathcal{M}} = \sqrt{\frac{1}{N_{\mathcal{M}}}\sum_{i=1}^{N_{\mathcal{M}}}\left(\frac{Q_{i,\mathcal{M}}^{\mathrm{MKT}} - Q_{i,\mathcal{M}}^{\mathrm{mdl}}}{Q_{i,\mathcal{M}}^{\mathrm{MKT}}}\right)^2}\ , \tag{14}$$

where $\mathcal{M} = \{\mathrm{SPX}, \mathrm{Fut}, \mathrm{VIX}\}$ denotes the market-specific label and $Q_{\mathcal{M}}^{\mathrm{MKT}}$ ($Q_{\mathcal{M}}^{\mathrm{mdl}}$) the market (model) quotes of the SPX (VIX) implied volatilities $\mathrm{IV}^{\mathrm{MKT}}$ ($\mathrm{IV}^{\mathrm{mdl}}$) and VIX futures prices F^{MKT} (F^{mdl}). Moreover, we evaluate the overall calibration performance with the aggregate errors[3]

$$\begin{aligned}\mathrm{RMSE}_{\mathrm{All}} &= \sqrt{\frac{1}{N}\sum_{\mathcal{M}}\sum_{i=1}^{N_{\mathcal{M}}}\left(Q_{i,\mathcal{M}}^{\mathrm{MKT}} - Q_{i,\mathcal{M}}^{\mathrm{mdl}}\right)^2}\ ,\\ \mathrm{RMSRE}_{\mathrm{All}} &= \sqrt{\frac{1}{N}\sum_{\mathcal{M}}\sum_{i=1}^{N_{\mathcal{M}}}\left(\frac{Q_{i,\mathcal{M}}^{\mathrm{MKT}} - Q_{i,\mathcal{M}}^{\mathrm{mdl}}}{Q_{i,\mathcal{M}}^{\mathrm{MKT}}}\right)^2}\ .\end{aligned} \tag{15}$$

where $N = N_{\mathrm{SPX}} + N_{\mathrm{Fut}} + N_{\mathrm{VIX}}$.

Table 4 reports average parameter estimates together with their in-sample standard deviation. Average parameters have sound economic interpretation, and they are in line with typical parameters found by the option pricing literature. Estimates indicate the presence of two volatility factors with approximate similar long-run mean ($\beta_1 \approx \beta_2$), with one factor being less persistent ($\alpha_2 > \alpha_1$) and more volatile ($\Lambda_2 > \Lambda_1$). The first factor has $\sigma_{1,0} \approx \sqrt{\beta_1}$, while the second has $\sigma_{2,0} < \sqrt{\beta_2}$, indicating a tendency of the volatility term structure to be increasing (through the second factor). Volatility shocks are virtually perfectly anticorrelated with the price shocks, indicating a strong leverage effect. Regarding price jumps, option prices reflect the fear of rare jumps (on average, $\lambda = 0.064$ for the Heston++ model, corresponding to a jump every 15 years) with a very large negative impact (-28% on average, with an average standard deviation of the jump size distribution of 41%, again for the Heston++ model). Volatility jumps have an average of 19.8% ($\mathcal{H}$) and 25.5% ($\mathcal{H}$++) for co-jumps (expressed in percentage, and as jumps in the volatility process), and of 22.7% for idiosyncratic jumps in the Heston++ model. Price and volatility co-jumps are also negatively correlated, providing a further statistical channel for the leverage effect. The frequency of idiosyncratic jumps appears to be smaller than that of co-jumps. Still, as discussed below, idiosyncratic jumps in volatility are not negligible from a pricing perspective. As usual, all parameters related to jumps are characterized by more uncertainty, as measured by the standard deviation of the parameters. Parameters related to the dynamics of the volatility factors are much less variable, in-sample, for the displaced Heston++ model with respect to the non-displaced Heston model.

Tables 5 reports the summary statistics on the root mean squared errors for the 2-SVCVJ and 2-SVCVJ++ models averaged over the three markets, while Tables 6, and 7, report the same summary statistics dissected on the three markets. The results clearly show that the addition of the deterministic shift is crucial for the joint fit of the three markets.

[3]In the definition of $\mathrm{RMSE}_{\mathrm{All}}$ we have divided by 100 each VIX futures price F in order to make it comparable with implied volatility levels IV.

Table 4: Calibrated parameters (annual units). This table reports the sample median (median absolute deviation) of joint SPX, VIX futures and VIX options calibrated parameters for the 2-SVCVJ and 2-SVCVJ++ models considered in the empirical analysis. The sample period is from January 7, 2009 to December 29, 2010 and the sampling frequency is weekly (Wednesdays). Panel A (B) reports 1^{st} (2^{nd}) volatility factor diffusive parameters. Panel C reports intensity and unconditional mean and standard deviation of normal jumps in price, where $\mathrm{E}[c_x] = \mu_x + \rho_J \mu_{co,\sigma}$ and $\mathrm{Var}[c_x] = \delta_x^2 + \rho_J^2 \mu_{co,\sigma}^2$ Panel D reports the correlated co-jumps parameters. The unconditional correlation between jump sizes is $\mathrm{corr}(c_x, c_\sigma) = \rho_J \mu_{co,\sigma} / \sqrt{\mathrm{Var}[c_x]}$. Panel E reports the idiosyncratic jumps parameters.

	2-SVCVJ		2-SVCVJ++	
Panel A: 1^{st} Factor				
α_1	1.967	(1.334)	1.676	(1.070)
$\sqrt{\beta_1}$ (%)	17.819	(9.162)	18.219	(6.079)
Λ_1	0.445	(0.219)	0.504	(0.115)
ρ_1	−0.865	(0.121)	−0.964	(0.036)
$\sigma_{1,0}$ (%)	16.250	(4.677)	16.376	(4.837)
Panel B: 2^{nd} Factor				
α_2	8.451	(3.420)	6.488	(2.477)
$\sqrt{\beta_2}$ (%)	22.950	(4.308)	21.531	(3.158)
Λ_2	2.050	(0.738)	2.115	(0.576)
ρ_2	−0.997	(0.003)	−1.000	(0.000)
$\sigma_{2,0}$ (%)	8.683	(6.309)	7.984	(4.640)
Panel C: Price jumps				
λ	0.079	(0.053)	0.064	(0.055)
$\mathrm{E}[c_x]$	−0.240	(0.151)	−0.280	(0.183)
$\sqrt{\mathrm{Var}[c_x]}$	0.318	(0.215)	0.413	(0.255)
Panel D: CO-jumps				
$\sqrt{\mu_{co,\sigma}}$ (%)	19.813	(19.808)	25.463	(25.014)
$\mathrm{corr}(c_x, c_\sigma)$	−0.363	(0.366)	−0.520	(0.458)
Panel E: Idiosyncratic jumps				
λ'	0.002	(0.002)	0.013	(0.012)
$\sqrt{\mu_{id,\sigma}}$ (%)	109.701	(106.420)	22.684	(21.928)

Table 5: Calibration errors (in %). This table reports the sample average (max in sample) of the Root Mean Squared Error (Panel A) and Root Mean Squared Relative Error (Panel B) of the 2-SVCVJ and 2-SVCVJ++ models calibrated jointly to SPX options, VIX futures and VIX options market data. The sample period is from January 7, 2009 to December 29, 2010 and the sampling frequency is weekly (Wednesdays). For each date in sample, the fit is performed minimizing the distance L in equation (12). Here we report the absolute (relative) errors on (S&P500 and VIX options) implied volatility surfaces $\mathrm{RMSE}_{\mathrm{SPX}}$ and $\mathrm{RMSE}_{\mathrm{VIX}}$ ($\mathrm{RMSRE}_{\mathrm{SPX}}$ and $\mathrm{RMSRE}_{\mathrm{VIX}}$) in percentage points and errors on the VIX futures term structures in US$. Performance measures are defined in equations (13) and (14). Overall pricing errors $\mathrm{RMSE}_{\mathrm{All}}$ and $\mathrm{RMSRE}_{\mathrm{All}}$ are expressed in percentage points and defined in equation (15).

	2-SVCVJ		2-SVCVJ++	
Panel A: RMSE				
$\mathrm{RMSE}_{\mathrm{SPX}}$	0.90	(4.28)	0.65	(1.64)
$\mathrm{RMSE}_{\mathrm{Fut}}$	0.53	(1.50)	0.22	(1.07)
$\mathrm{RMSE}_{\mathrm{VIX}}$	3.39	(14.70)	1.64	(4.03)
$\mathrm{RMSE}_{\mathrm{All}}$	1.42	(4.57)	0.82	(2.11)
Panel B: RMSRE				
$\mathrm{RMSRE}_{\mathrm{SPX}}$	3.07	(11.31)	2.02	(3.95)
$\mathrm{RMSRE}_{\mathrm{Fut}}$	1.81	(6.13)	0.74	(2.60)
$\mathrm{RMSRE}_{\mathrm{VIX}}$	4.78	(23.56)	2.04	(4.34)
$\mathrm{RMSRE}_{\mathrm{All}}$	3.34	(10.70)	2.01	(3.94)

Table 6: Calibration RMSRE (in %) on SPX options by Moneyness - Maturity category. This table reports the sample average of the Root Mean Squared Relative Error for different Moneyness and time-to-Maturity categories of S&P500 options for the 2-SVCVJ (Panel A) and 2-SVCVJ++ (Panel B) models calibrated jointly to S&P500 options, VIX futures and VIX options market data. The sample period is from January 7, 2009 to December 29, 2010 and the sampling frequency is weekly (Wednesdays). For each date in sample, the fit is performed minimizing the distance L in equation (12). Here we report the relative errors on S&P500 implied volatility surfaces RMSE_{SPX}, as defined in (14), conditioned to the Moneyness - Maturity category considered. Time to *Maturity* is measured in days and *Moneyness* for an option is defined as the ratio of the option exercise price to the current index level: low, ATM and high moneyness are defined by *Moneyness* < 0.95, $0.95 - 1.05$, and > 1.05, respectively. For each category, errors are expressed in percentage points and the sample average is weighted by the number of daily observations in each category. Overall errors are reported in Table 5

.

Maturity	**Moneyness**							
	Panel A: 2-SVCVJ model				**Panel B**: 2-SVCVJ++ model			
	low	ATM	high	**All**	low	ATM	high	**All**
< 45	3.00	3.68	4.34	3.60	2.23	2.12	3.06	2.42
$45 - 90$	1.88	1.68	2.27	2.01	1.62	0.90	1.64	1.53
> 90	2.11	3.16	4.48	3.27	1.65	1.43	2.40	1.93
All	2.49	3.10	3.83		1.93	1.67	2.40	
	Panel C: Observations				**Panel D**: Observations (% of TOT)			
	low	ATM	high	**All**	low	ATM	high	**All**
< 45	4,232	2,642	1,373	8,247	17.43	10.88	5.66	33.97
$45 - 90$	4,704	2,368	2,292	9,364	19.37	9.75	9.44	38.57
> 90	3,369	1,418	1,881	6,668	13.88	5.84	7.75	27.46
All	12,305	6,428	5,546	24,279	50.68	26.48	22.84	100.00

To better illustrate matters, Figure 1 shows the calibration of the 2-SVCVJ++ and 2-SVCVJ models on a specific day in which the VIX futures display a hump[4], that is of the models with the largest number of parameters, with and without the deterministic shift extension. The figure shows, quite clearly, that taking advantage of the added flexibility provided by the deterministic shift ϕ_t in fitting the term structure of VIX futures, the proposed model (solid red) is able to calibrate vanilla and VIX options jointly without particular difficulty. The "traditional" affine model (dashed blue), missing such a flexibility, cannot calibrate the prices of the two market even if the number of parameters is quite high (17). Figure 2 shows the same exercise on a day in which the non-displaced model is able to reproduce the VIX futures term structure, but not the VIX options. In this case, the flexibility of the displacement is used by the Heston++ model to fit the rapidly declining term structure of the VIX options implied volatility.

The non-displaced Heston model performs on average with a sample mean relative error of 3.1% on SPX vanilla options, 1.8% on VIX futures and 4.8% on VIX options. Still, as shown in Figure 1, it often fails in reproducing a humped VIX futures term structure and, as confirmed by Table 7, it tends to perform poorly at longer maturities. As further shown in Table 6, the calibration error on vanilla options on S&P500 tends to increase, in absolute terms, at short and long maturities and as moneyness increases.

With the simple introduction of the displacement ϕ_t, which is costless from a computational perspective, the three relative errors mentioned above become 2.0%, 0.7%, and 2.0% respectively. In terms of absolute average root mean square error (see Table 5), this implies a gain of 28% on vanilla options, which was already documented by Pacati et al. (2014) on FX vanilla options. On top of that, we show a much larger advantage on VIX futures (-58%) and VIX options (-52%). Thus, the deterministic shift extension is even

[4]Figures corresponding to al 104 calibrations are available upon request from the authors.

Table 7: Calibration RMSRE (in %) on VIX options by Moneyness - Maturity category and VIX futures by tenor. This table reports the sample average of the Root Mean Squared Relative Error for different Moneyness and time-to-Maturity categories of call options on VIX and VIX Futures for the 2-SVCVJ (Panel A) and 2-SVCVJ++ (Panel B) models calibrated jointly to S&P500 options, VIX futures and VIX options market data. The sample period is from January 7, 2009 to December 29, 2010 and the sampling frequency is weekly (Wednesdays). For each date in sample, the fit is performed minimizing the distance L in equation (12). Here we report the relative errors on VIX implied volatility surfaces $\text{RMSRE}_{\text{VIX}}$ and VIX Futures term structure $\text{RMSRE}_{\text{Fut}}$, as defined in (14), conditioned to the Moneyness - Maturity category considered and tenor bucket, respectively. Time to *Maturity* is measured in days and *Moneyness* for an option of maturity T is defined as the ratio of the exercise price to the current VIX futures price expiring at T; ITM, ATM and OTM for calls are defined by *Moneyness* < 1.0, $1.0 - 1.4$, and > 1.4, respectively. For each category, errors are expressed in percentage points and the sample average is weighted by the number of daily observations in each category. Overall errors are reported in Table 5.

Maturity	**Moneyness**									
	Panel A: 2-SVCVJ model					**Panel B**: 2-SVCVJ++ model				
	Options				Futures	Options				Futures
	ITM	ATM	OTM	**All**		ITM	ATM	OTM	**All**	
< 45	6.12	3.58	3.28	4.67	0.35	1.85	1.85	2.02	2.08	0.12
$45 - 90$	7.93	2.81	3.00	5.19	0.21	1.84	1.81	2.15	2.11	0.13
> 90	6.87	3.14	2.88	4.73	1.07	1.69	1.96	2.06	2.00	0.44
All	7.61	3.41	3.15			1.90	2.03	2.17		
	Panel C: Observations					**Panel D**: Observations (% of TOT)				
	Options				Futures	Options				Futures
	ITM	ATM	OTM	**All**		ITM	ATM	OTM	**All**	
< 45	160	194	230	584	144	5.78	7.01	8.31	21.11	18.18
$45 - 90$	220	202	302	724	144	7.95	7.30	10.91	26.17	18.18
> 90	447	525	487	1,459	504	16.15	18.97	17.60	52.73	63.64
All	827	921	1,019	2,767	792	29.89	33.29	36.83	100.00	100.00

more important on variance derivatives, where the average estimation error is more than halved with respect to the traditional benchmark. It is particularly striking that the *maximum* absolute error of the Heston++ model becomes 3.9%, 2.6% and 4.3% respectively, which is comparable with the *average* error obtained without displacement. On VIX options, the maximum error with displacement is even less than the average error without displacement.[5] The maximum overall absolute pricing error $\text{RMSRE}_{\text{All}}$ is instead 10.70% for the Heston model.[6]

From this in-sample exercise we can clearly see that both kind of jumps in volatility (idiosyncratic and correlated to price jumps) are needed to calibrate effectively, providing indirect evidence for the presence of both in the volatility dynamics. To gain insight, we only consider models endowed with the displacement, and we compare the decrease in average absolute pricing error with respect to the model without jumps in volatility, the 2-SVJ++. Overall, adding only idiosyncratic jumps in volatility or adding correlated jumps

[5]These results are obtained without imposing the Feller condition. We have performed the same calibration imposing the Feller condition $2\alpha_i\beta_i \geq \Lambda_i^2$ separately on each volatility factor ($i = 1, 2$) (Duffie and Kan, 1996; Andersen and Piterbarg, 2007). With this restriction imposed, the average (maximum) relative pricing error of Heston++ increase to 4% (11.7%) on SPX options, 4.4% (12%) on VIX options and 1.4% (5.6%) on VIX futures, while for the Heston model we obtained 4.9% (22.1%) on SPX options, 7.3% (25.4%) on VIX options and 2.5% (5.8%) on VIX futures. Thus, imposing the Feller condition does not affect the superiority of the extension. Pacati et al. (2015) discuss the theoretical and empirical reasons to relax the Feller condition; see also the discussion in Song and Xiu (2016); Amengual and Xiu (2018).

[6]When the Feller condition is imposed, the mean (maximum) overall relative pricing error $\text{RMSRE}_{\text{All}}$ grows up to 5.23% (20.92%) for the Heston model and 4.05% (11.63%) for the Heston++ model. Again, there is a strong benefit in relaxing the Feller condition.

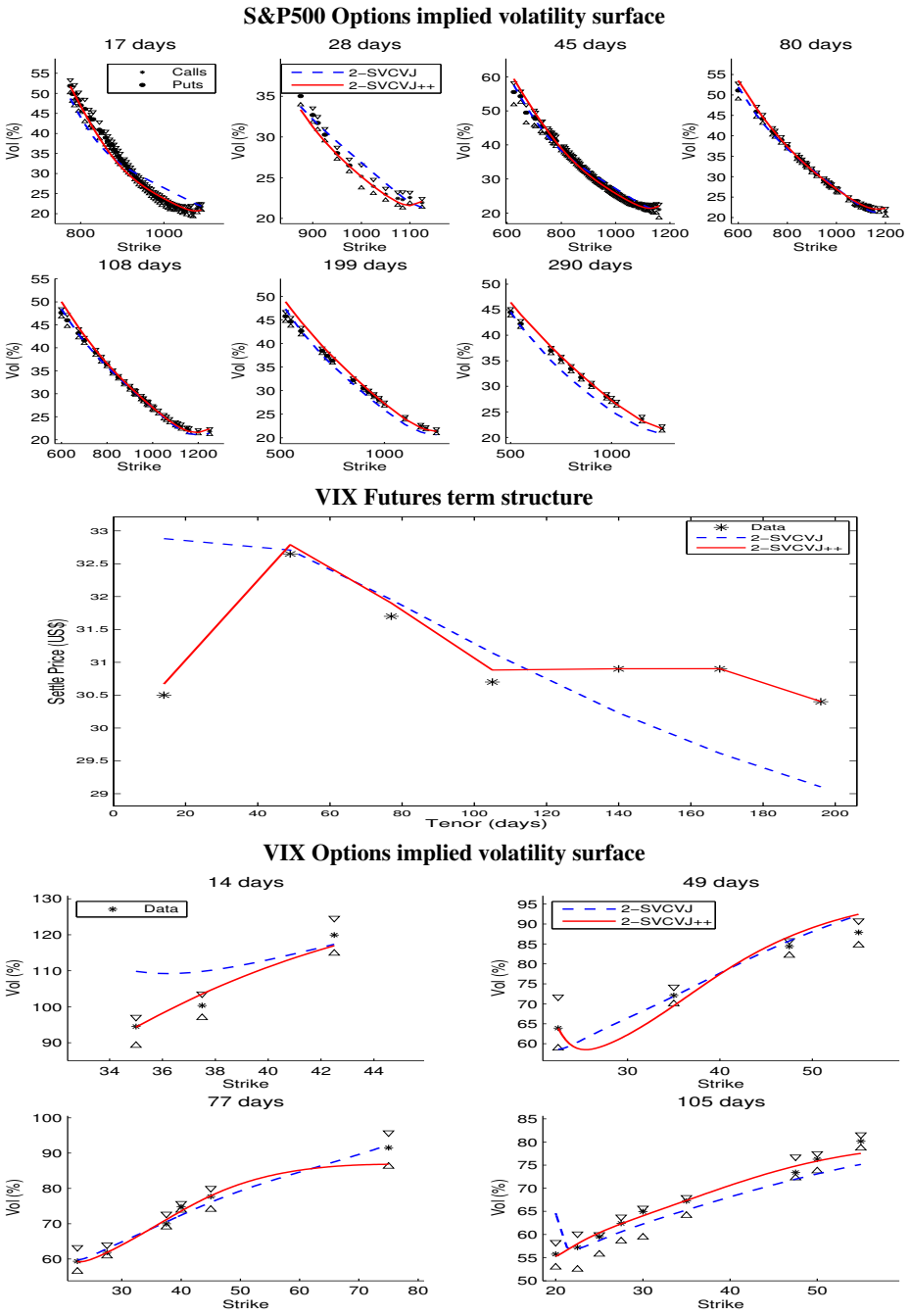

Figure 1: This figure reports market and model implied volatilities for S&P500 (plot at the top) and VIX (plot at the bottom) options, together with the term structure of VIX futures (plot in the middle) on September 2, 2009 obtained calibrating jointly on the three markets the 2-SVCVJ (blue dashed line) and 2-SVCVJ++ (red line). Maturities and tenors are expressed in days and volatilities are in % points and VIX futures settle prices are in US$.

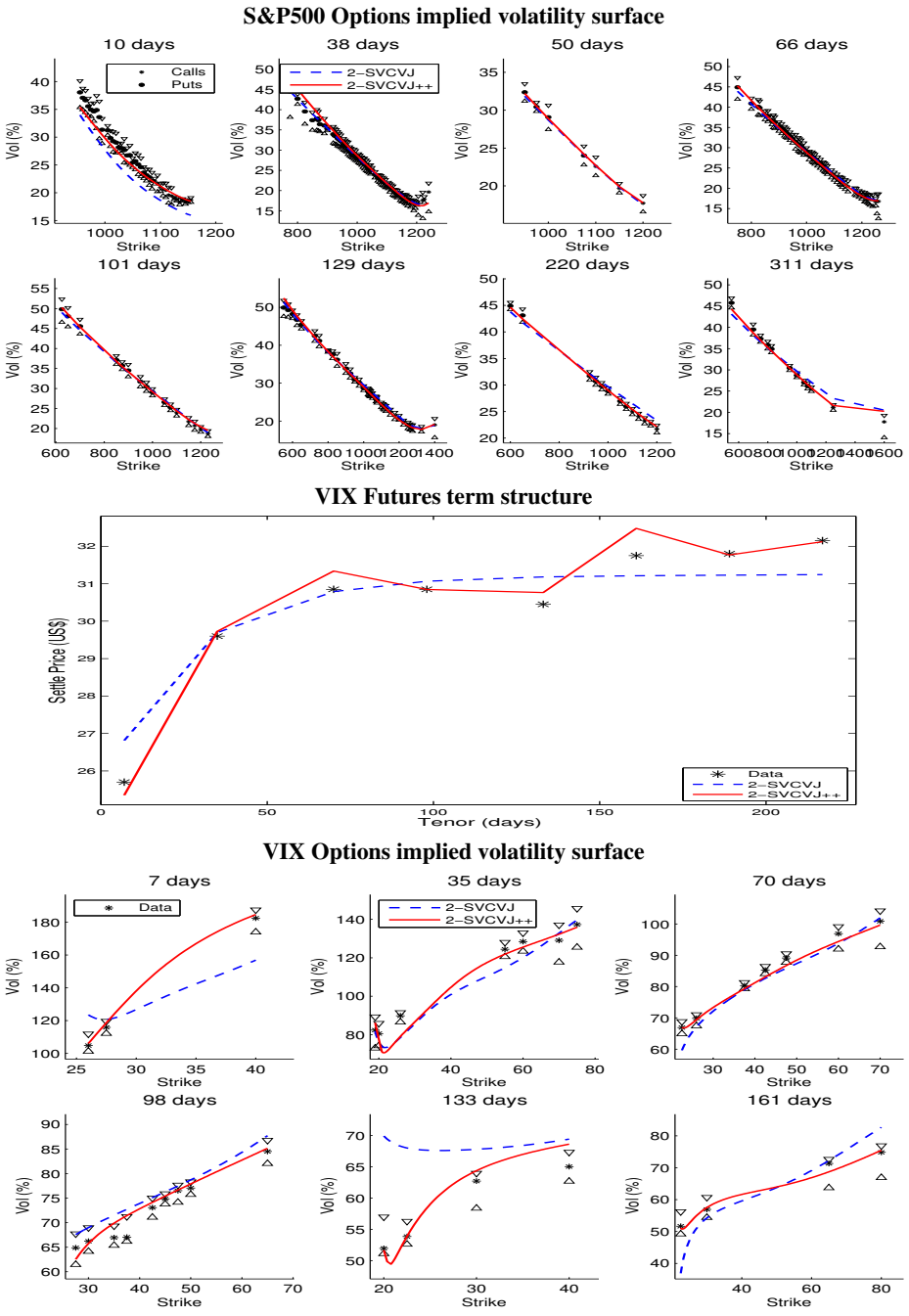

Figure 2: This figure reports market and model implied volatilities for S&P500 (plot at the top) and VIX (plot at the bottom) options, together with the term structure of VIX futures (plot in the middle) on August 11, 2010 obtained calibrating jointly on the three markets the 2-SVCVJ (blue dashed line) and 2-SVCVJ++ (red line). Maturities and tenors are expressed in days and volatilities are in % points and VIX futures settle prices are in US$.

produces the same calibration advantage with respect to the model without volatility jumps: −26% for correlated jumps, −31% for idiosyncratic jumps. Adding both volatility jumps yields a gain of −47%. The larger effect is on VIX options (−57%) and VIX futures (−55%). Consistently with the intuition that jumps have larger impact on short terms, the gain (again with respect to the 2-SVJ++, but now in terms of the relative errors) is −65% on VIX options with maturity shorter than 45 days, −52% on VIX options with maturity between 45 and 90 days, and −43% on VIX options with maturity longer than 90 days. Thus, the impact of both kind of idiosyncratic jumps is larger on short term VIX options.

As one may argue, this better fit of the displaced Heston++ model might simply be a consequence of having a larger number of parameters. To investigate this issue, we compared the Heston and Heston++ models for each day using a likelihood ratio test, under the assumption of homoskedastic Normally distributed and independent errors and considering as additional parameters of the nesting specification the piecewise integrals of the displacement (see Appendix B.1).[7] For each calibrated day, the test p-value is less than 1%, implying therefore strong statistical support for the displaced model.[8]

After having discussed the statistical significance of the displacement, in the next Section we turn to examining the improvements in the hedging and out-of-sample cross-sectional pricing performance induced by its introduction.

4. Hedging performance and out-of-sample pricing

Does the addition of a deterministic displacement to the volatility dynamics improves hedging performance? To answer this question, we assume that the options analyzed so far, both on S&P500 and VIX are hedged using a strategy meant to neutralize the three main sources of risk: shocks to the underlying price and to the two volatility factors. Specifically, we hedge options using a portfolio composed of three instruments: the underlying asset S_t, and two VIX futures, the one with the shortest available maturity above the week, F_t^{short}, and the one with the longest available maturity below the year, F_t^{long}. The choice of two futures with different maturity, meant two account for a two-factor volatility risk, allows to hedge changes in the variance level and in the slope of the variance term structures. Specifically, given an option with price O_t (either on S&P500 or VIX), the replicating portfolio is given by:

$$V_t^O = \Delta \cdot S_t + \beta_{short} \cdot F_t^{short} + \beta_{long} \cdot F_t^{long} + \text{cash}$$

[7] To this end, the loss function of both models was rewritten as the sum of $N = N_{\text{SPX}} + N_{\text{Fut}} + N_{\text{VIX}}$ squared errors ε_ℓ

$$L = \sum_{\ell=1}^{N} \varepsilon_\ell^2 = \sum_{i=1}^{N_{\text{SPX}}} \left(\frac{1}{\sqrt{N_{\text{SPX}}}} - \frac{\text{IV}^{\text{mdl}}_{i,\text{SPX}}}{\text{IV}^{\text{MKT}}_{i,\text{SPX}} \sqrt{N_{\text{SPX}}}} \right)^2 + \sum_{j=1}^{N_{\text{Fut}}} \left(\frac{1}{\sqrt{N_{\text{Fut}}}} - \frac{F^{\text{mdl}}_j}{F^{\text{MKT}}_j \sqrt{N_{\text{Fut}}}} \right)^2 + \sum_{k=1}^{N_{\text{VIX}}} \left(\frac{1}{\sqrt{N_{\text{VIX}}}} - \frac{\text{IV}^{\text{mdl}}_{k,\text{VIX}}}{\text{IV}^{\text{MKT}}_{k,\text{VIX}} \sqrt{N_{\text{VIX}}}} \right)^2 .$$

Assuming the same variance V_ε for each error, our calibration becomes a maximum likelihood estimate, with log-likelihood

$$-\frac{N}{2} \log(2\pi) - \frac{1}{2} \sum_{\ell=1}^{N} \left[\log V_\varepsilon + \frac{\varepsilon_\ell^2}{V_\varepsilon} \right] = -\frac{N}{2} \log(2\pi V_\varepsilon) - \frac{1}{2V_\varepsilon} L \ .$$

[8] Alternatively, the Akaike Information criterion (AIC) ranking yields the same outcome.

where the "hedge ratios" Δ, β_{short}, and β_{long} are determined by imposing risk-neutrality with respect to the three risk factors, namely:

$$\begin{aligned}
&\frac{\partial O_t}{\partial S}(S_t, \sigma_{1,t}^2, \sigma_{2,t}^2) = \Delta \ , \\
&\frac{\partial O_t}{\partial \sigma_1^2}(S_t, \sigma_{1,t}^2, \sigma_{2,t}^2) = \beta_{short}\frac{\partial F_t^{short}}{\partial \sigma_1^2}(S_t, \sigma_{1,t}^2, \sigma_{2,t}^2) + \beta_{long}\frac{\partial F_t^{long}}{\partial \sigma_1^2}(S_t, \sigma_{1,t}^2, \sigma_{2,t}^2) \ , \\
&\frac{\partial O_t}{\partial \sigma_2^2}(S_t, \sigma_{1,t}^2, \sigma_{2,t}^2) = \beta_{short}\frac{\partial F_t^{short}}{\partial \sigma_2^2}(S_t, \sigma_{1,t}^2, \sigma_{2,t}^2) + \beta_{long}\frac{\partial F_t^{long}}{\partial \sigma_2^2}(S_t, \sigma_{1,t}^2, \sigma_{2,t}^2) \ ,
\end{aligned} \tag{16}$$

where, of course, $\Delta = 0$ for VIX options. The quantity of cash needed for the hedging portfolio is determined by the requirement $V_t^O = O_t$.

Hedging performance is evaluated as follows. For each option in our data used for calibration (Wednesday options) with at least 7 days of maturity, we compute numerically the Greeks needed in Eq. (16) to recover the hedging quantities Δ, β_{short}, and β_{long}.[9] Then, for a horizon h ranging from 1 to 5 market days (that is from the following Thursday to the following Wednesday), we compute the percentage return of the option

$$r_h^O = \frac{O_{t+h} - O_t}{O_t} \ ,$$

using the market value of O_{t+h}, and of the corresponding hedging portfolio return

$$r_h^{\mathcal{P}} = \frac{V_{t+h}^O - V_t^O}{V_t^O} \ ,$$

using market values of S_{t+h}, F_{t+h}^{short} and F_{t+h}^{long}. The hedging performs well when r_h^O is close to $r_h^{\mathcal{P}}$. Therefore, our measure of performance is the difference between these two returns. Our hedging exercise is meant to be realistic, since it uses three suitable instruments to hedge three risk factors, and cost-effective since we use the same instruments for all options, either on S&P500 or VIX. Moreover, it represents a truly out-of-sample metric of the model performance, since the hedging portfolio is composed at time t using the calibrated parameters (to compute the Greeks), and the hedging performance is evaluated on following days using realized market values.

Figure 3 reports quantiles and mean absolute deviations of the hedging error, defined as MAD = median $\left|r_h^{\mathcal{P}} - r_h^O\right|$. The figure shows that the addition of the displacement yields significant improvements in the hedging performance of both SPX and VIX options, and especially for the former. In particular, hedging with the traditional 2-SVCVJ model (without displacement) could generate large outliers in the hedging error distribution. On the contrary, hedging errors are much more contained using the displacement. Tables 8 and 9 reports the absolute hedging errors at the rebalancing horizons considered. For SPX options (Table 8), the hedging improvement is more or less uniform across strikes and maturities. For VIX options (Table 9) the improvement is particularly relevant for options with low moneyness, while there is some deterioration for options with large moneyness.

Finally, we proceed to a genuine out-of-sample pricing exercise, inspired by a similar exercise in Bakshi et al. (1997). For out-of-sample pricing, indeed, the additional presence of the displacement may actually cause overfitting and have the 2-SVCVJ++ model penalized if the extra parameters do not improve the model

[9] In this exercise, we converted puts to calls using put-call-parity.

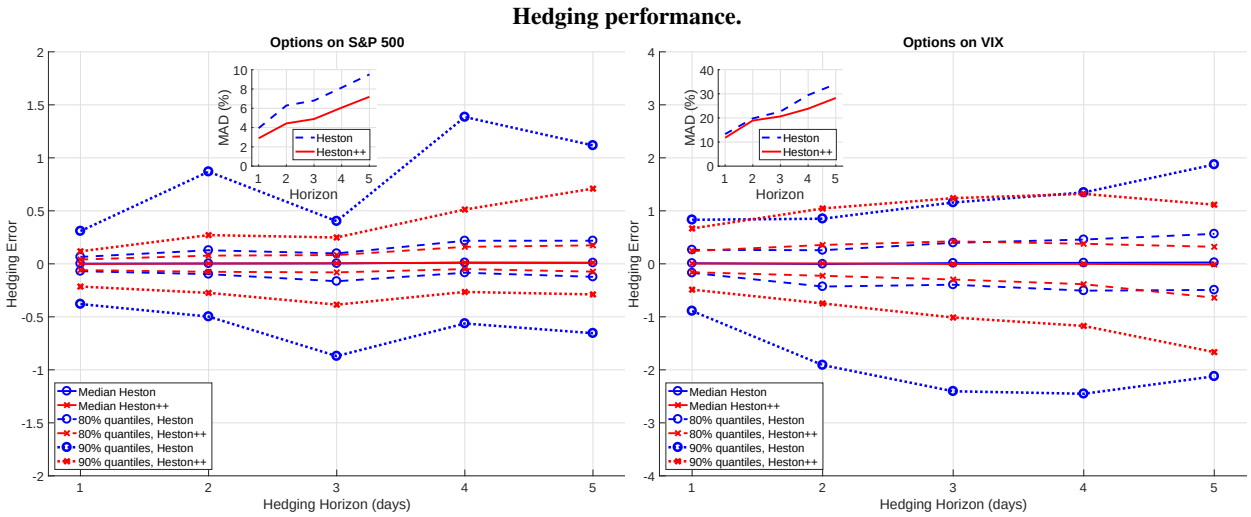

Figure 3: Reports quantiles of the hedging error $r_h^{\mathcal{P}} - r_h^{\mathcal{O}}$ on S&P 500 options (left panel) and VIX options (right panel), for the 2-SVCVJ (labeled Heston) and the 2-SVCVJ++ (labeled Heston++) model. In the insets the mean absolute deviation MAD = median$|r_h^{\mathcal{P}} - r_h^{\mathcal{O}}|$, where $r_h^{\mathcal{P}}$ is the percentage return, over the given horizon h, on the hedging portfolio and $r_h^{\mathcal{O}}$ is the corresponding return of the hedged option.

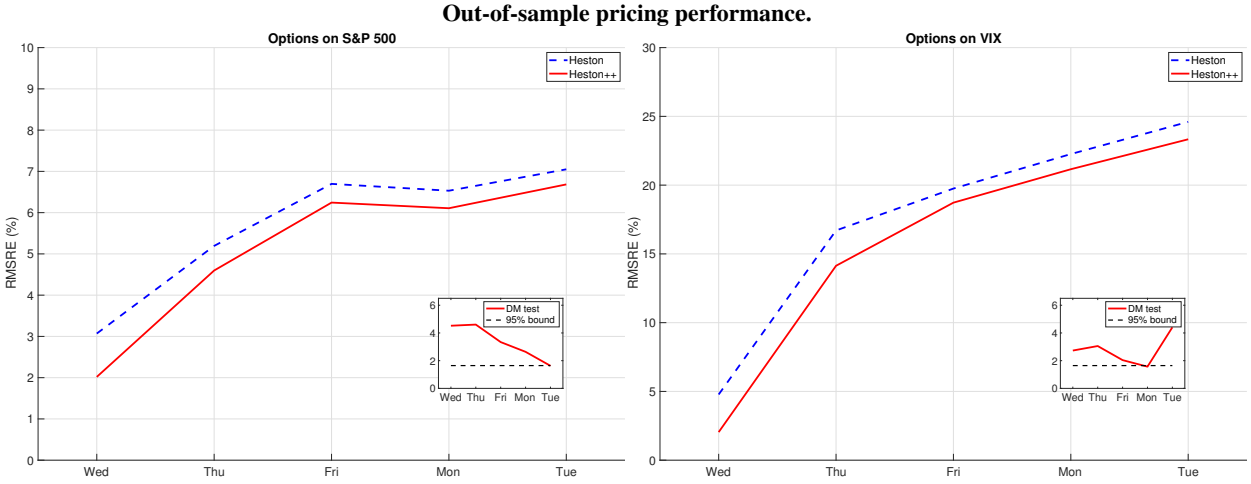

Figure 4: Reports the out-of-sample average RMSRE of option pricing using the 2-SVCVJ (labeled Heston) and the 2-SVCVJ++ (labeled Heston++) model, for SPX options (left panel) and VIX options (right panel). The models are calibrated on Wednesdays, so the first point in the figure is the in-sample RMSRE, as reported in Table 5. Then, these parameters are used as input for pricing in the following days. The insets report Diebold-Mariano tests for superior out-of-sample pricing of the Heston++ model, using the average MSRE as the loss function.

specification. In this exercise, we rely on parameters calibrated on each Wednesday, and use them as input to compute option prices on the following days.[10] Figure 4 shows the out-of-sample pricing performance, in terms of average RMSRE for SPX and VIX options. The first point in the figures corresponds to the in-sample RMSRE, as reported in Table 5. Clearly, as we move forward in time, the pricing performance of the "frozen"

[10]The displacement at time $t + h$ is obtained by linearly interpolating the term structure calibrated at date t. Details are provided in Appendix B.2.

Table 8: Hedging errors (in %) on SPX call options by Moneyness - Maturity category. This table reports the median absolute hedging error MAD = median$|r_h^{\mathcal{P}} - r_h^{\mathcal{Q}}|$ for different Moneyness and time-to-Maturity categories for the 2-SVCVJ (Panel A) and the 2-SVCVJ++ (Panel B) models. The hedging horizons range from 1 (following Thursday) to 5 (next Wednesday) business days and hedged options range from 16256 (1 day horizon) to 13826 (5 days horizon). Time to *Maturity* is measured in days and *Moneyness* is defined as the ratio of the exercise price to the current index level; ITM, ATM and OTM for calls are defined by *Moneyness* < 0.95, $0.95 - 1.05$, and > 1.05, respectively. Maturity/Moneyness buckets are defined and fixed at the time in which the replicating portfolio is formed.

Maturity	**Moneyness**							
	Panel A: 2-SVCVJ model				**Panel B**: 2-SVCVJ++ model			
	ITM	ATM	OTM	**All**	ITM	ATM	OTM	**All**
Thursday								
< 45	2.40	12.66	34.56	7.80	1.80	9.60	26.85	5.48
$45 - 90$	1.57	4.73	17.57	3.65	1.25	3.64	13.16	2.84
> 90	0.66	1.95	11.77	1.70	0.52	2.02	8.14	1.43
All	1.43	6.06	19.30	3.94	1.10	4.71	14.09	2.89
Friday								
< 45	3.51	23.75	69.16	11.47	2.50	14.37	59.23	7.78
$45 - 90$	2.49	6.89	38.14	5.98	1.72	5.67	24.20	4.31
> 90	0.90	3.25	21.99	2.56	0.73	3.04	14.73	2.08
All	2.17	10.13	38.21	6.29	1.58	7.37	25.69	4.43
Monday								
< 45	4.21	22.95	59.31	13.71	3.05	15.73	42.55	8.07
$45 - 90$	2.85	7.70	48.91	6.90	2.31	6.81	36.35	5.34
> 90	1.14	3.82	29.05	3.19	0.92	3.67	20.11	2.36
All	2.41	9.48	43.21	6.80	1.91	7.79	32.20	4.89
Tuesday								
< 45	5.12	29.09	72.94	17.35	3.69	22.24	65.01	11.32
$45 - 90$	3.38	9.31	56.75	7.50	2.66	8.78	42.42	6.19
> 90	1.19	4.87	23.57	3.44	1.02	4.92	18.13	2.82
All	2.74	13.57	47.72	8.14	2.17	10.63	36.30	6.07
Wednesday								
< 45	7.08	37.10	150.61	23.12	5.49	28.42	109.77	16.79
$45 - 90$	3.64	10.89	61.22	9.43	2.84	10.24	45.13	7.61
> 90	1.16	4.79	29.14	3.76	1.10	5.03	21.04	2.95
All	3.01	13.40	53.69	9.51	2.43	11.63	42.43	7.19

parameters deteriorates. However, the Heston++ remains superior to the Heston model even out-of-sample. The out-of-sample superiority of the Heston++ model is significant, as assessed by a Diebold-Mariano test which uses the average MSRE as the loss function (we use one lag in the implementation of the test), as displayed in Figure 4.[11] This result, in connection with the lower variability of parameters related to the volatility factors documented in Section 3, justifies the superior hedging performance of the displaced Heston++ model with respect to the non-displaced counterpart.

5. The role of the displacement

The novelty of the proposed approach in this paper is the introduction of the deterministic displacement ϕ_t, which thus deserves a separate discussion. We recall that, in our calibration exercise, no functional form

[11] A Diebold-Mariano test on the superiority of the hedging performance of the Heston++ model is instead not significant. This is due to the large outliers in hedging errors of the 2-SVCVJ model documented in Figure 3.

Table 9: Hedging errors (in %) on VIX call options by Moneyness - Maturity category. This table reports the median absolute hedging error MAD = median$|r_h^{\mathcal{P}} - r_h^{\mathcal{Q}}|$ for different Moneyness and time-to-Maturity categories for the 2-SVCVJ (Panel A) and the 2-SVCVJ++ (Panel B) models. The hedging horizons range from 1 (following Thursday) to 5 (next Wednesday) business days and hedged call options range from 985 (1 day horizon) to 917 (5 days horizon). Time to *Maturity* is measured in days and *Moneyness* for an option of maturity T is defined as the ratio of the exercise price to the VIX futures price expiring at T; ITM, ATM and OTM for calls are defined by *Moneyness* < 1.0, 1.0 − 1.4, and > 1.4, respectively. Maturity/Moneyness buckets are defined and fixed at the time in which the replicating portfolio is formed.

Maturity	**Moneyness**							
	Panel A: 2-SVCVJ model				**Panel B**: 2-SVCVJ++ model			
	ITM	ATM	OTM	**All**	ITM	ATM	OTM	**All**
Thursday								
< 45	15.18	81.19	115.78	66.44	8.00	78.65	146.37	55.93
45 – 90	7.20	20.25	28.59	18.39	4.74	19.72	46.41	17.34
> 90	6.85	7.79	12.68	9.38	4.80	7.92	17.88	8.49
All	8.72	13.46	23.69	13.29	5.62	10.86	33.49	11.78
Friday								
< 45	17.41	119.17	150.17	81.69	15.38	116.22	112.40	73.11
45 – 90	10.77	18.87	44.33	21.07	6.04	20.52	72.46	20.79
> 90	11.03	10.44	17.65	13.20	9.67	9.88	20.01	12.62
All	11.54	17.67	36.64	19.79	9.26	15.86	45.68	18.92
Monday								
< 45	27.52	121.19	271.96	88.80	19.38	120.46	211.58	72.57
45 – 90	12.43	37.74	59.90	34.56	7.35	34.86	84.29	33.01
> 90	11.37	12.28	22.33	14.31	8.19	11.14	24.05	13.60
All	13.22	21.77	43.53	22.65	9.04	23.78	48.94	20.63
Tuesday								
< 45	32.71	118.84	161.72	89.47	25.60	118.25	225.71	83.00
45 – 90	18.22	42.20	68.42	42.20	12.79	43.55	77.13	37.31
> 90	13.82	15.95	23.27	16.87	11.62	16.36	28.97	15.64
All	17.84	30.39	49.10	29.47	13.70	26.48	54.08	23.83
Wednesday								
< 45	38.54	144.52	231.41	127.77	26.44	175.29	225.05	123.39
45 – 90	27.26	45.67	61.85	45.36	16.55	44.96	91.80	42.07
> 90	17.95	17.17	32.84	21.11	17.71	20.43	41.07	21.91
All	22.55	27.91	54.66	34.07	18.10	29.07	76.23	28.28

is assumed for the displacement and only its integrals are estimated. This is consistent e.g. with a piecewise constant ϕ_t across the maturities of the considered derivatives. We start by showing, in Figure 5, the dynamics (right panel) and the average estimate (left panel), across the 104 weeks, of

$$\sigma_\phi(0,T) = 100 \cdot \sqrt{\frac{1}{T} I_\phi(0,T)} \ , \tag{17}$$

where $I_\phi(t,T) = \int_t^T \phi_s ds$. The purpose of the transformation in Eq. (17) is to express the displacement in the same units of the VIX index, making its interpretation easier. Figure 5 shows that the contribution of the displacement is substantial, hovering around $4 - 11\%$ across different weeks and maturities, with a median value around 7% almost flat across maturities.

We now discuss the interpretation of these estimates, as well as their time series properties. We concentrate on the minimum value, implied by the model, which the forward VIX can realize in the risk-neutral world.

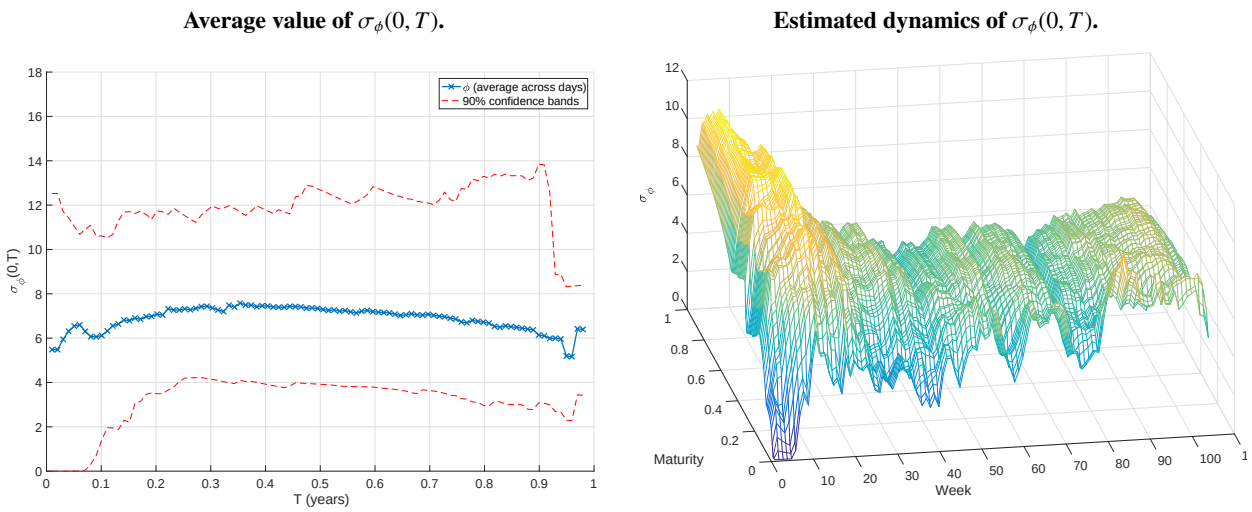

Figure 5: Left panel: average estimate of $\sigma_\phi(0,T) = 100 \cdot \sqrt{\frac{1}{T} I_\phi(0,T)}$, as a function of the maturity T, across the 104 days fitted in the time span 2009–2010. Right panel: estimated dynamics of $\sigma_\phi(0,T)$ over time (we use an exponential smoother with lag 10 weeks).

Looking at the proof of Proposition 2 in the appendix, this is easily given by:

$$\begin{aligned}\left(\frac{\mathrm{VIX}_t^{\min}}{100}\right)^2 = &\sum_{k=1,2} \beta_k \left(\bar\tau - \frac{1-e^{-\bar\tau\alpha_k}}{\alpha_k}\right) && \text{(volatility drift contribution)}\\ &+ \frac{\lambda\mu_{co,\sigma}+\lambda'\mu_{id,\sigma}}{\alpha_1}\left(\bar\tau - \frac{1-e^{-\bar\tau\alpha_1}}{\alpha_1}\right) + \bar\mu - (\mu_x+\rho_J\mu_{co,\sigma}) && \text{(jumps contribution)}\\ &+ \frac{1}{\bar\tau} I_\phi(t, t+\bar\tau) && \text{(displacement contribution),}\end{aligned} \tag{18}$$

where $\bar\tau = 1$ month, which can be computed given the calibrated parameters. This quantity is composed of three parts: the first two (volatility drift and jumps contribution) denote the contribution to the minimum from the "vibrancy" of the underlying volatility, and are the only ones determining the minimum in traditional affine models. The third part (displacement contribution) is specific to the Heston++ models, and allows the minimum of the forward VIX to depend on the maturity. Without the displacement, the attainable minimum of the forward VIX is the same for all maturities.

Figure 6 reports the time series of model-implied values of the forward VIX, that is $\mathrm{VIX}^{\min}$ in Eq. (18), at maturities 1 and 6 months for the 2-SVCVJ and 2-SVCVJ++ model, together with the respective displacement contribution. The figure makes clear what is the contribution of the displacement in this setting. The model-implied attainable minimum coincides in the Heston and in the Heston++ case. This is to be expected since this quantity depends on the calibration of the two models on the very same option surfaces. However, in the non-displaced case, the calibration of the lower value attainable by the VIX is done using the available parameters, see Eq. (18), which restricts their ability to match high-order moments of the risk-neutral distribution.

Clearly, higher moments of the risk-neutral distribution are also affected by ϕ_t. To show this, Figure 7 reports the impact of the displacement ϕ on the moments of the forward VIX distribution (at 6 months maturity), computed as calculated in Proposition 4 in the Appendix. We use average parameter estimates.

Time series of $\mathrm{VIX}^{\min}$.

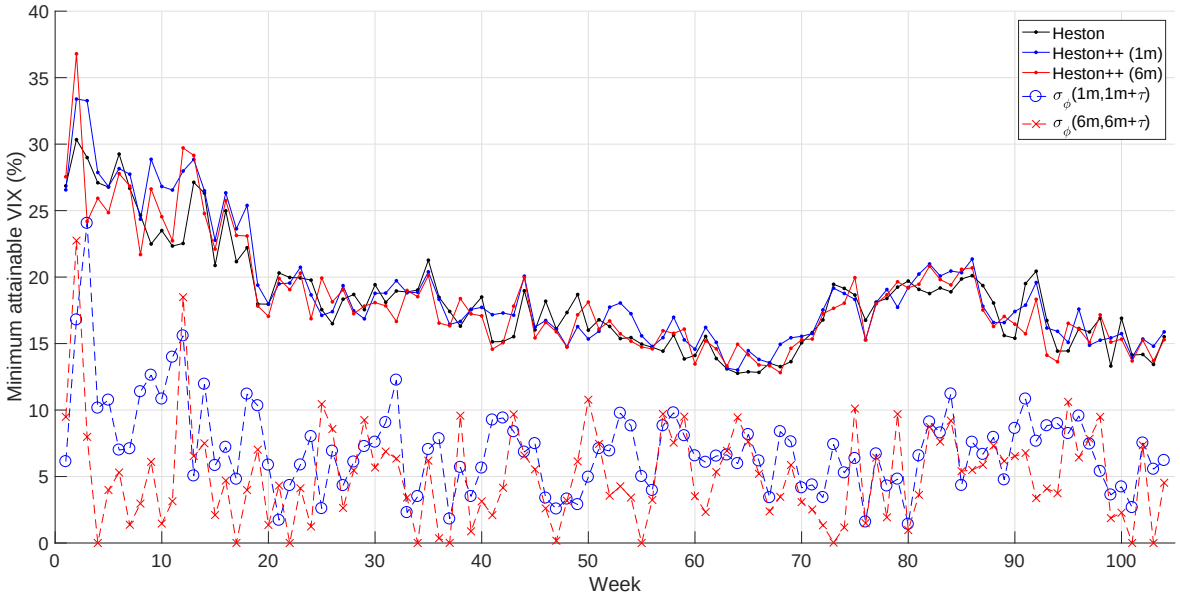

Figure 6: Reports the time series of model implied forward VIX minimum, computed with formula (18), for the Heston and the Heston++ models (solid lines). Note that for the traditional affine models the minimum is constrained to be the same for all maturities. The figure also reports the contribution of the displacement to this term (dashed lines). The sample spans 104 weeks in 2009 and 2010.

We consider the case $\phi_t = c$ for increasing values of c (the value $c = 0$ corresponding to the case without displacement). We report the displacement in terms of $\sigma_\phi(0, 6m) = 100\sqrt{c}$. The figure makes clear that the displacement has an intuitive effect on VIX moments, an higher ϕ_t corresponding to higher mean, lower standard deviation, higher skewness and higher kurtosis. In this sense, the displacement contributes to non-Gaussianities which are strongly required to generate a positive variance premium, and, at the same time, reliable out-of-the-money derivatives pricing, see the discussion in Bakshi et al. (2003) and, more recently, Bekaert and Engstrom (2017). In Table 10, we report the average and standard deviation of weekly model-implied risk neutral moments at different horizons. The difference between calibrated third and fourth moments is striking, with the Heston++ model providing smaller and more stable high-order moments.

We can thus interpret the displacement as a "VIX shift" that can be used to push the (risk-neutral) distribution of the forward VIX up. Providing an artificial lower bound, expressed in terms of displacement, is empirically sensible since the VIX has an historical lower bound: the lowest close value of the VIX has been 9.14% on November 3, 2017. It thus makes then sense that traders do expect a lower bound for the forward volatility. The added flexibility to the risk-neutral distribution resulting from the "volatility shift" due to the displacement explains the superior pricing performance of Heston++ models. The computational cost of the addition is negligible, since by using a deterministic displacement the model is still in the affine class.

Finally, Figure 8 compares the dynamics of $\sigma_\phi(0, 6m)$ (a mid-term average displacement, see again Figure 5) to the dynamics of the variance risk premium. The variance risk premium on day t (VRP_t)

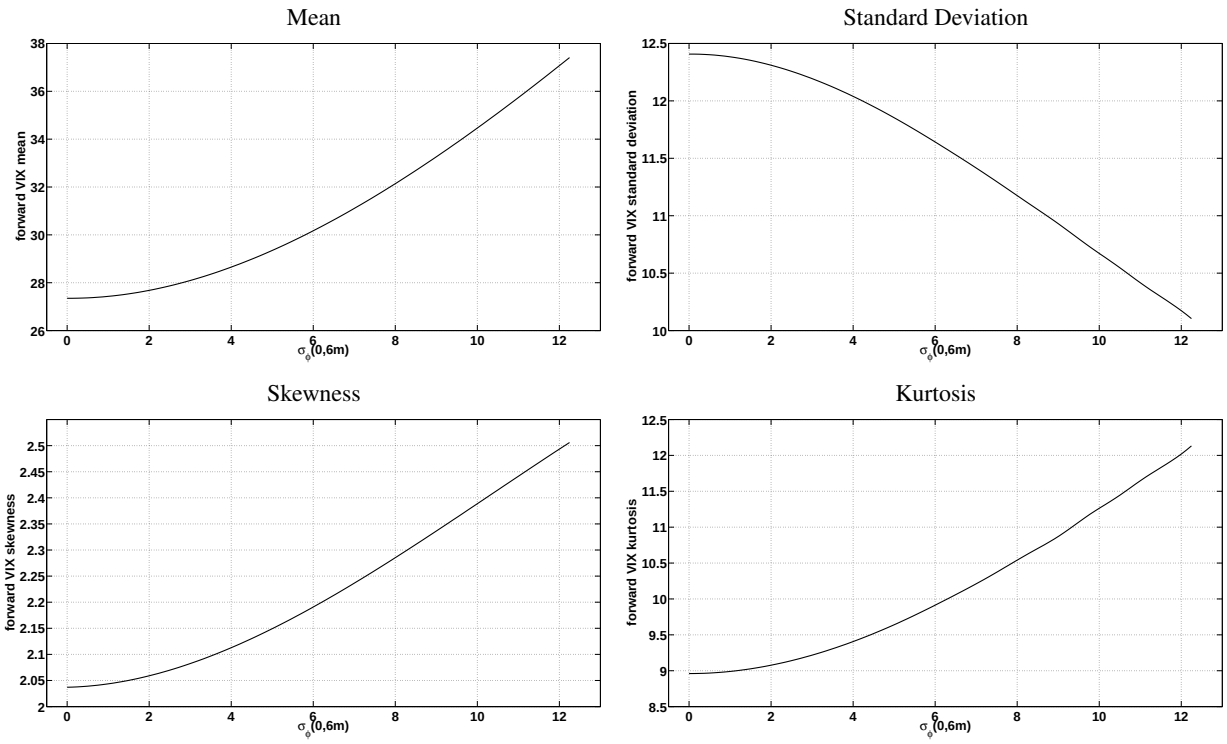

Figure 7: Reports the moments of the forward VIX distribution at 6 months maturity in the case $\phi_t = c$, as a function of $\sigma_\phi(0, 6m) = 100\sqrt{c}$ for various values of the coefficient c.

corresponding to the horizon τ is defined as:

$$\left(\frac{\mathrm{VRP}_t}{100}\right)^2 = \mathrm{E}^{\mathbb{Q}}\left[\mathrm{QV}(t, t+\tau)\right] - \mathrm{E}^{\mathbb{P}}\left[\mathrm{QV}(t, t+\tau)\right] \quad , \tag{19}$$

where $\mathrm{E}^{\mathbb{Q}}\left[\mathrm{QV}(t, t+\tau)\right]$ is the expected *risk-neutral* quadratic variation of the stock index between times t and $t+\tau$, and $\mathrm{E}^{\mathbb{P}}\left[\mathrm{QV}(t, t+\tau)\right]$ is the expected quadratic variation in the same interval. We use $\tau = 1$ month and we estimate VRP_t using:

$$\widehat{\mathrm{VRP}_t} = \mathrm{VIX}^2_{t,t+30} - \widetilde{\mathrm{RV}}_{t,t+30} \quad , \tag{20}$$

where $\mathrm{VIX}_{t,t+30}$ is the 30-days VIX index observed on day t, and $\widetilde{\mathrm{RV}}_{t,t+30} = e^{\widehat{\log \mathrm{RV}_{t,t+30}}}$ is the forecasted realized variance as obtained from the regression:

$$\log \mathrm{RV}_{t,t+30} = \alpha_0 + \alpha_1 \log \mathrm{VIX}^2_{t-1,t+29} + \alpha_2 \log \mathrm{RV}_{t-30,t-1} + \alpha_3 \log \mathrm{RV}_{t-90,t-1} + \varepsilon_t \quad , \tag{21}$$

where ε_t is noise and

$$\mathrm{RV}_{t,t+h} = 252 \cdot \psi \cdot \sum_{t \le t' \le t+h} \mathrm{RV}_{t'} \quad ,$$

with $\mathrm{RV}_{t'}$ being the 5-minutes open-to-close realized variance on day t, properly rescaled by 252 (to convert it to yearly units) and by the constant ψ, which is the ratio between the sum of squared close-to-close S&P500 daily returns and the average of RV in the sample, and which is meant to take into account the contribution

Table 10: Model-implied risk neutral moments of the forward VIX distribution at 1, 3, 6 months and 1 year horizons for the Heston and Heston++ model. Reported values are median (median absolute deviation) over the 104 weekly calibrations of the models. Panel A reports the mean, Panel B the standard deviation, Panel C the skewness and Panel D the kurtosis. Model implied moments are calculated as described in Proposition 4 in the Appendix.

	2-SVCVJ		2-SVCVJ++	
Panel A: Mean				
1 month	27.47	(4.15)	26.78	(4.26)
3 months	29.27	(3.09)	29.10	(3.12)
6 months	29.56	(2.50)	29.38	(2.62)
1 year	29.43	(2.76)	29.42	(2.69)
Panel B: Standard Deviation				
1 month	8.88	(2.13)	7.80	(1.90)
3 months	12.62	(2.78)	11.28	(2.01)
6 months	14.24	(2.48)	13.11	(2.15)
1 year	15.56	(2.98)	14.10	(2.58)
Panel C: Skewness				
1 month	6.09	(4.08)	3.05	(0.76)
3 months	3.94	(1.88)	2.97	(0.45)
6 months	4.02	(1.84)	2.82	(0.56)
1 year	4.09	(2.01)	2.78	(0.76)
Panel D: Kurtosis				
1 month	101.29	(92.01)	21.08	(9.30)
3 months	44.51	(35.36)	17.98	(5.84)
6 months	39.11	(30.00)	15.92	(5.15)
1 year	37.67	(29.40)	14.98	(6.53)

of overnight returns to the total variance. The model (21) is a modification of the model used in Caporin et al. (2017) to include the lagged VIX as a regressor, as suggested by Bekaert and Hoerova (2014) (and indeed highly significant in our sample). The figure clearly shows a common pattern in the dynamics of the two objects, with a correlation above 50%. This common pattern could be explained either by the interpretation of the displacement as an additional volatility factor, useful to add flexibility not only in the matching of the risk-neutral forward VIX moments but also of its minimum, or by a "support risk premium", or a combination of both. Indeed, as made clear by the literature (see e.g. Section 8 in Bandi and Renò, 2016 and the discussion therein) a time varying variance risk premium can be obtained even with time invariant preferences. This makes the identification of the relative contribution of the displacement to the dynamics of the risk premia and/or the volatility state as difficult as for the other volatility factors.[12] This said, our results are compatible with the behavior of traders who use the displacement as a heuristic correction of affine models meant to adjust their aggregate perception of changing risk premia.

Summarizing, this section provides a palatable interpretation of the displacement ϕ_t, which is the main novelty introduced by this paper. The displacement is, mathematically, a "forward VIX push-up", that is a contribution to the lower bound of the risk-neutral probability density function of the forward VIX, allowing it to vary with the maturity. Empirically, the effect is sizable. We can thus explain the successful pricing performance due to the introduction of the displacement in the Heston++ model as follows. The displacement is used by the model to bound the dynamics of the VIX leaving free the other parameters, especially jump parameters, to match the higher moments of the risk-neutral distribution, e.g. enhancing the fit of the slope of

[12]Notice that the interpretation of the displacement as a volatility factor is purely qualitative here, since the displacement is deterministic, and in this sense it is inherently different from a volatility factor. Making it deterministic, however, is exactly the trick adopted in this paper to gain flexibility in affine models.

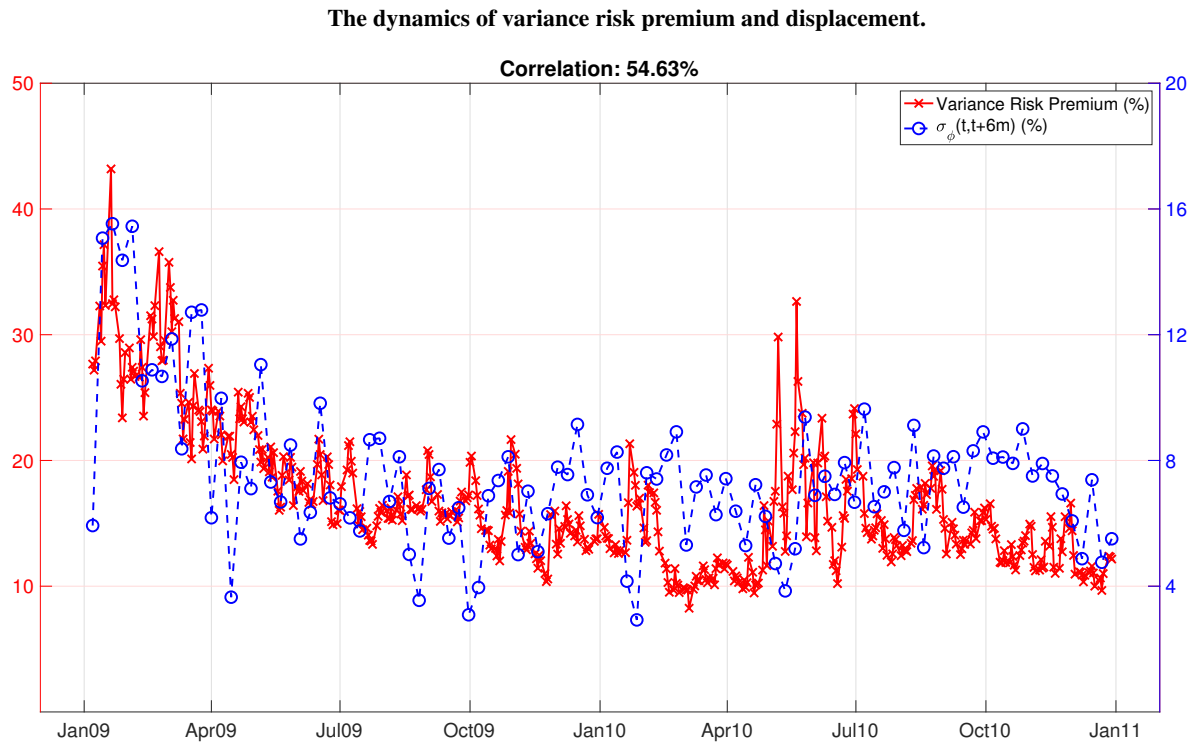

Figure 8: Reports the time series of the estimated variance risk premium VRP_t, and of $\sigma_\phi(t, t+6m)$.

the VIX options (Sepp, 2008b). This leads to much better pricing of VIX derivatives, without compromising the quality of the fit on vanilla options. The bound to the forward VIX is empirically sensible (the VIX never gets too low) and is compatible with the interpretation of the displacement as a "support risk premium", that is as a minimal value added to true volatility expectations when pricing variance derivatives.

6. Conclusions

This paper calibrates jointly S&P 500 vanilla options and VIX futures and options with average relative discrepancy from market prices of 2%, and maximum relative discrepancy of 4% by means of the Heston++ model, an affine two-factor model with jumps endowed with a deterministic shift extension (the displacement). The deterministic shift extensions is showed to play a crucial role in easing the calibration of the term structure of both VIX futures and options, and to have a sound interpretation as a forward VIX shift, supported by the data. The improvement in the option fitting is statistically significant, carries over out-of-sample, and determines a sizable improvement of the hedging performance of the options. The data also show that the displacement is highly correlated with the dynamics of the variance risk premium. Assessing whether the displacement should be interpreted as an additional (deterministic) volatility factor and/or as a support risk premium requires the specification of the dynamics of the Heston++ model under the natural probability $\mathbb{P}$, in addition to the dynamics under the risk-neutral probability $\mathbb{Q}$, and the estimation of this joint dynamics, which is left for future research.

Further, the calibration exercise suggests that two kind of jumps are present in the volatility dynamics, the first being independent from jumps in price, and the second being correlated with them, that is happening at the same time and with anti-correlated size. The impact of both jumps is particularly beneficial on short

term VIX options, and their importance is not affected by the presence of the displacement.

Importantly, the Heston++ models achieve these performances without any additional computational costs with respect to traditional benchmarks. This observation makes these models ideal candidates for the joint calibration of volatility surfaces.

Acknowledgments

We would like to thank two anonymous reviewers, the associate editor and the editor Geert Bekaert, as well as participants to the XVI and XVII Workshop on Quantitative Finance held in Parma and in Scuola Normale Superiore, Pisa respectively. We finally thank the IMT of Lucca for providing financial support. All errors and omissions remain our own.

Appendix A. Mathematical appendix

Conditional characteristic functions of $\mathcal{H}$ models. As the 2-SVCVJ is an affine model, ordinary calculations following Duffie et al. (2000) lead to characteristic functions which are exponentially affine in the state variables. For the logarithmic price and volatility factors we obtain, respectively:

$$\begin{aligned}
\log f_x^{\text{2-SVCVJ}}(z;\tau) &= i(x_t + (r-q)\tau)z + \sum_{k=1,2}\left(A_k^x(z;\tau) + B_k^x(z;\tau)\sigma_{k,t}^2\right) + C_{co}^x(z;\tau) + C_{id}^x(z;\tau) \ , \\
\log f_\sigma^{\text{2-SVCVJ}}(z_1,z_2;\tau) &= \sum_{k=1,2}\left(A_k^\sigma(z_k;\tau) + B_k^\sigma(z_k;\tau)\sigma_{k,t}^2\right) + C_{co}^\sigma(z_1;\tau) + C_{id}^\sigma(z_1;\tau) \ ,
\end{aligned} \tag{A.1}$$

where coefficients satisfy the following sets of ODEs:

$$\begin{aligned}
\frac{\partial A_k^x(z;\tau)}{\partial\tau} &= \alpha_k\beta_k B_k^x(z;\tau) \ , \\
\frac{\partial B_k^x(z;\tau)}{\partial\tau} &= \frac{1}{2}\Lambda_k^2\left(B_k^x(z;\tau)\right)^2 - (\alpha_k - iz\rho_k\Lambda_k)\,B_k^x(z;\tau) - \frac{1}{2}z(i+z) \ , \\
\frac{\partial C_{co}^x(z;\tau)}{\partial\tau} &= \lambda\Big(\theta^{co}\left(z,-iB_1^x(z,\tau)\right) - 1 - i\bar{\mu}z\Big) \ , \\
\frac{\partial C_{id}^x(z;\tau)}{\partial\tau} &= \lambda'\Big(\theta^{id}\left(-iB_1^x(z,\tau)\right) - 1\Big) \ ,
\end{aligned}$$

with null initial conditions at $\tau = 0$, and

$$\begin{aligned}
\frac{\partial A_k^\sigma(z_k;\tau)}{\partial\tau} &= \alpha_k\beta_k B_k^\sigma(z_k;\tau) \ , \\
\frac{\partial B_k^\sigma(z_k;\tau)}{\partial\tau} &= \frac{1}{2}\Lambda_k^2\left(B_k^\sigma(z_k;\tau)\right)^2 - \alpha_k B_k^\sigma(z_k;\tau) \ , \\
\frac{\partial C_{co}^\sigma(z_1;\tau)}{\partial\tau} &= \lambda\Big(\theta^{co}\left(0,-iB_1^\sigma(z_1,\tau)\right) - 1\Big) \ , \\
\frac{\partial C_{id}^\sigma(z_1;\tau)}{\partial\tau} &= \lambda'\Big(\theta^{id}\left(-iB_1^\sigma(z_1,\tau)\right) - 1\Big) \ ,
\end{aligned} \tag{A.2}$$

with initial conditions $A_k^\sigma(z_k;0) = C_{co}^\sigma(z_1;0) = C_{id}^\sigma(z_1;0) = 0$ and $B_k^\sigma(z_k;0) = iz_k$. Explicit solutions can be found. For the $f_x^{\text{2-SVCVJ}}$ coefficients, we have:

$$
\begin{aligned}
A_k^x(z;\tau) &= \frac{\alpha_k\beta_k}{\Lambda_k^2}\left[(c_k - d_k)\tau - 2\log\left(\frac{1-g_k e^{-d_k\tau}}{1-g_k}\right)\right] \ , \\
B_k^x(z,\tau) &= \frac{c_k - d_k}{\Lambda_k^2}\frac{1-e^{-d_k\tau}}{1-g_k e^{-d_k\tau}} \ , \\
C_{co}^x(z;\tau) &= \lambda\tau\Big(\Theta^{co}(z;\tau) - 1 - i\bar{\mu}z\Big) \ , \\
\Theta^{co}(z;\tau) &= exp\left\{i\mu_x z - \frac{1}{2}\delta_x^2 z^2\right\} \ , \\
&\quad \times \frac{1}{G_{co}^-}\left[1 - \frac{2}{\tau}\frac{\mu_{co,\sigma}}{\Lambda_1^2}\frac{1}{G_{co}^+}\log\left(\frac{G_{co}^- - g_1 G_{co}^+ e^{-d_1\tau}}{(1-g_1)(1-iz\rho_J\mu_{co,\sigma})}\right)\right] \ , \\
C_{id}^x(z;\tau) &= \lambda'\tau\Big(\Theta^{id}(z;\tau) - 1\Big) \ , \\
\Theta^{id}(z;\tau) &= \frac{1}{G_{id}^-}\left[1 - \frac{2}{\tau}\frac{\mu_{id,\sigma}}{\Lambda_1^2}\frac{1}{G_{id}^+}\log\left(\frac{G_{id}^- - g_1 G_{id}^+ e^{-d_1\tau}}{1-g_1}\right)\right] \ ,
\end{aligned}
$$

where we have defined the auxiliary parameters:

$$
\begin{aligned}
c_k &= \alpha_k - iz\rho_k\Lambda_k \ , \\
d_k &= \sqrt{c_k^2 + z(i+z)\Lambda_k^2} \ , \\
g_k &= \frac{c_k - d_k}{c_k + d_k} \ , \\
G_{co}^\pm &= 1 - iz\rho_J\mu_{co,\sigma} - \frac{\mu_{co,\sigma}}{\Lambda_1^2}(c_1 \pm d_1) \ , \\
G_{id}^\pm &= 1 - \frac{\mu_{id,\sigma}}{\Lambda_1^2}(c_1 \pm d_1) \ .
\end{aligned}
$$

For the $f_\sigma^{\text{2-SVCVJ}}$ coefficients, we have:

$$
\begin{aligned}
A_k^\sigma(z_k;\tau) &= -\frac{2\alpha_k\beta_k}{\Lambda_k^2}\log\left(1 - iz_k\frac{\Lambda_k^2}{2\alpha_k}(1-e^{-\alpha_k\tau})\right) \ , \\
B_k^\sigma(z_k;\tau) &= \frac{iz_k e^{-\alpha_k\tau}}{1 - iz_k\frac{\Lambda_k^2}{2\alpha_k}(1-e^{-\alpha_k\tau})} \ , \\
C_{co}^\sigma(z_1;\tau) &= \lambda\Theta(z_1;\tau,\mu_{co,\sigma}) \ , \\
C_{id}^\sigma(z_1;\tau) &= \lambda'\Theta(z_1;\tau,\mu_{id,\sigma}) \ , \\
\Theta(z_1;\tau,\mu) &= -\frac{2\mu}{\Lambda_1^2 - 2\alpha_1\mu}\log\left(1 - \frac{iz_1}{1-iz_1\mu}\frac{\Lambda_1^2 - 2\alpha_1\mu}{2\alpha_1}(1-e^{-\alpha_1\tau})\right) \ .
\end{aligned}
\tag{A.3}
$$

Characteristic functions of the other nested $\mathcal{H}$ models can be obtained applying the appropriate simplifications to the corresponding expressions just presented for the 2-SVCVJ model, as discussed in section (2.1), see Lian and Zhu (2013) and Kokholm and Stisen (2015) for the case of the SVCJ model of Duffie et al. (2000)

and Chen and Poon (2013) for the case of the 2-SVCJ model with two volatility factors with correlated co-jumps between the first one and the price process. We present here the expressions for the nested models adopted in the empirical analysis. For ease of exposition we begin with the results for the two factor continuous 2-SV model of Christoffersen et al. (2009):

$$\begin{aligned} \log f_x^{\text{2-SV}}(z;\tau) &= i(x_t + (r-q)\tau)z + \sum_{k=1,2}\left(A_k^x(z;\tau) + B_k^x(z;\tau)\sigma_{k,t}^2\right) \ , \\ \log f_\sigma^{\text{2-SV}}(z_1,z_2;\tau) &= \sum_{k=1,2}\left(A_k^\sigma(z_k;\tau) + B_k^\sigma(z_k;\tau)\sigma_{k,t}^2\right) \ . \end{aligned} \tag{A.4}$$

For the 2-SVJ model, with log-normal jumps in price only we obtain:

$$\begin{aligned} \log f_x^{\text{2-SVJ}}(z;\tau) &= \log f_x^{\text{2-SV}}(z;\tau) + C_{co}^x(z;\tau)\Big|_{\mu_{co,\sigma}=0} \ , \\ \log f_\sigma^{\text{2-SVJ}}(z_1,z_2;\tau) &= \log f_\sigma^{\text{2-SV}}(z_1,z_2;\tau) \ . \end{aligned} \tag{A.5}$$

For the 2-SVVJ model, with log-normal jumps in price and idiosyncratic jumps in $\sigma_{1,t}^2$ we obtain:

$$\begin{aligned} \log f_x^{\text{2-SVVJ}}(z;\tau) &= \log f_x^{\text{2-SVJ}}(z;\tau) + C_{id}^x(z;\tau) \ , \\ \log f_\sigma^{\text{2-SVVJ}}(z_1,z_2;\tau) &= \log f_\sigma^{\text{2-SV}}(z_1,z_2;\tau) + C_{id}^\sigma(z_1;\tau) \ . \end{aligned} \tag{A.6}$$

For the 2-SVCJ model, with correlated co-jumps in price and $\sigma_{1,t}^2$ we obtain:

$$\begin{aligned} \log f_x^{\text{2-SVCJ}}(z;\tau) &= \log f_x^{\text{2-SV}}(z;\tau) + C_{co}^x(z;\tau) \ , \\ \log f_\sigma^{\text{2-SVCJ}}(z_1,z_2;\tau) &= \log f_\sigma^{\text{2-SV}}(z_1,z_2;\tau) + C_{co}^\sigma(z_1;\tau) \ . \end{aligned} \tag{A.7}$$

Relations (5) are easily derived since each $\mathcal{H}$++ model is an affine model nesting the corresponding undisplaced $\mathcal{H}$ model. □

Proof of Proposition 1. The pricing formula is easily obtained from the first of (5) and from a straightforward application of results of Lewis (2000, 2001). □

Proof of Proposition 2. Applying Itō's Lemma to the process $\log(S_{t+\bar\tau}/F_{t,t+\bar\tau})$, under the dynamics of the 2-SVCVJ++ in (1), the VIX definition in (7) may be rewritten as

$$\left(\frac{\text{VIX}_t}{100}\right)^2 = \frac{1}{\bar\tau}\sum_{k=1,2}\mathrm{E}^{\mathbb{Q}}\left[\int_t^{t+\bar\tau}\sigma_{k,s}^2 ds \,\middle|\, \mathcal{F}_t\right] + 2\lambda\,\mathrm{E}^{\mathbb{Q}}\left[e^{c_x} - 1 - c_x\right] + \frac{1}{\bar\tau}I_\phi(t,t+\bar\tau) \ , \tag{A.8}$$

where we have also used the fact that ϕ_t is a deterministic function. The integrated volatilities and the co-jumps contribution can be computed in closed form (see for example Lin (2007) and Duan and Yeh (2010) for similar computations)

$$\begin{aligned} \mathrm{E}^{\mathbb{Q}}\left[\int_t^{t+\bar\tau}\sigma_{1,s}^2 ds \,\middle|\, \mathcal{F}_t\right] &= \frac{1-e^{-\bar\tau\alpha_1}}{\alpha_1}\sigma_{1,t}^2 + \frac{\alpha_1\beta_1 + \lambda\mu_{co,\sigma} + \lambda'\mu_{id,\sigma}}{\alpha_1}\left(\bar\tau - \frac{1-e^{-\bar\tau\alpha_1}}{\alpha_1}\right) \ , \\ \mathrm{E}^{\mathbb{Q}}\left[\int_t^{t+\bar\tau}\sigma_{2,s}^2 ds \,\middle|\, \mathcal{F}_t\right] &= \frac{1-e^{-\bar\tau\alpha_2}}{\alpha_2}\sigma_{2,t}^2 + \beta_2\left(\bar\tau - \frac{1-e^{-\bar\tau\alpha_2}}{\alpha_2}\right) \ , \\ \mathrm{E}^{\mathbb{Q}}\left[e^{c_x} - 1 - c_x\right] &= \bar\mu - (\mu_x + \rho_J\mu_{co,\sigma}) \ , \end{aligned} \tag{A.9}$$

and therefore we have that the coefficients of affinity in (9) are

$$
\begin{aligned}
a_k(\bar{\tau}) &= \frac{1-e^{-\bar{\tau}\alpha_k}}{\alpha_k} \quad , \quad k=1,2, \\
b_1(\bar{\tau}) &= \frac{\alpha_1\beta_1 + \lambda\mu_{co,\sigma} + \lambda'\mu_{id,\sigma}}{\alpha_1}\Big(\bar{\tau} - a_1(\bar{\tau})\Big) + 2\lambda\bar{\tau}\Big[\bar{\mu} - (\mu_x + \rho_J\mu_{co,\sigma})\Big] \ , \\
b_2(\bar{\tau}) &= \beta_2\Big(\bar{\tau} - a_2(\bar{\tau})\Big) \ .
\end{aligned}
\tag{A.10}
$$

Relation (8) readily comes from the nesting of 2-SVCVJ model into 2-SVCVJ++ if $\phi_t \equiv 0$. □

Proof of Proposition 3. The payoffs of a VIX futures contract settled at time T and of a call option on VIX of strike K maturing at T are linear functions of the VIX index value at settle VIX_T, respectively VIX_T and $(\mathrm{VIX}_T - K)^+$. As stated in Proposition 2, under $\mathcal{H}$++ models, VIX_T is non-linearly related to the value of volatility factor processes at time T, whose conditional characteristic function is known in closed form as shown in Lemma 1. To overcome this issue we rewrite the payoffs as non-linear functions of the squared index

$$
\begin{aligned}
\frac{w_F(\mathrm{VIX}'^2_T)}{100} &= \sqrt{\mathrm{VIX}'^2_T} \ , \\
\frac{w_C(\mathrm{VIX}'^2_T)}{100} &= \left(\sqrt{\mathrm{VIX}'^2_T} - K'\right)^+ \ ,
\end{aligned}
\tag{A.11}
$$

where $\mathrm{VIX}'_t = \mathrm{VIX}_t/100$ and $K' = K/100$ are, respectively, the index and strike values expressed in percentage points. Fourier transforms for these payoffs are available in closed form

$$
\begin{aligned}
\frac{\hat{w}_F(z)}{100} &= \frac{\sqrt{\pi}}{2}\frac{1}{(-iz)^{3/2}} \ , \\
\frac{\hat{w}_C(z)}{100} &= \frac{\sqrt{\pi}}{2}\frac{1-\mathrm{erf}(K'\sqrt{-iz})}{(-iz)^{3/2}} \ ,
\end{aligned}
\tag{A.12}
$$

and are single-valued regular functions in the upper half of the complex plane

$$
\mathbb{S}_w = \{z \in \mathbb{C} : \mathrm{Im}(z) > 0\} \quad . \tag{A.13}
$$

Denote with $f^{\text{2-SVCVJ++}}_{\mathrm{VIX}'^2}$ the time t conditional characteristic function $\mathrm{E}^{\mathbb{Q}}\left[e^{iz\,\mathrm{VIX}'^2_T} \,\middle|\, \mathcal{F}_t\right]$ of the squared index process VIX'^2_t at time T under the 2-SVCVJ++ model. From Proposition 2 (with $\tau = T - t$)

$$
\begin{aligned}
f^{\text{2-SVCVJ++}}_{\mathrm{VIX}'^2}(z;\tau) &= e^{izI_\phi(T,T+\bar{\tau})/\bar{\tau}} f^{\text{2-SVCVJ}}_{\mathrm{VIX}'^2}(z;\tau) \\
&= e^{iz\left(\sum_{k=1,2} b_k(\bar{\tau}) + I_\phi(T,T+\bar{\tau})\right)/\bar{\tau}} f^{\text{2-SVCVJ}}_{\sigma}\left(za_1(\bar{\tau})/\bar{\tau}, za_2(\bar{\tau})/\bar{\tau};\tau\right)
\end{aligned}
\tag{A.14}
$$

Following the approach of (Lewis, 2000, 2001), the value at time t of the call option on VIX under the 2-SVCVJ++ model is given by

$$
\begin{aligned}
C^{\text{2-SVCVJ++}}_{\mathrm{VIX}}(K,t,T) &= e^{-r\tau}\,\mathrm{E}^{\mathbb{Q}}\left[(\mathrm{VIX}_T - K)^+ \,\middle|\, \mathcal{F}_t\right] = e^{-r\tau}\,\mathrm{E}^{\mathbb{Q}}\left[w_C(\mathrm{VIX}'^2_T) \,\middle|\, \mathcal{F}_t\right] \\
&= \frac{e^{-r\tau}}{2\pi}\int_{i\,\mathrm{Im}(z)-\infty}^{i\,\mathrm{Im}(z)+\infty} f^{\text{2-SVCVJ++}}_{\mathrm{VIX}'^2}(-z;\tau)\hat{w}_C(z)dz \ ,
\end{aligned}
\tag{A.15}
$$

and similarly for futures

$$F_{\text{VIX}}^{\text{2-SVCVJ++}}(t,T) = \mathrm{E}^{\mathbb{Q}}\left[\,\text{VIX}_T \mid \mathcal{F}_t\right] = \mathrm{E}^{\mathbb{Q}}\left[\,w_F(\text{VIX}_T'^2)\,\middle|\,\mathcal{F}_t\right] \\ = \frac{1}{2\pi}\int_{i\,\text{Im}(z)-\infty}^{i\,\text{Im}(z)+\infty} f_{\text{VIX}'^2}^{\text{2-SVCVJ++}}(-z;\tau)\hat{w}_F(z)dz \ , \tag{A.16}$$

from which the results in Proposition 3 follow since the real (imaginary) part is an even (odd) function of $\text{Re}(z)$. For both claims, the integrands are well behaved functions as long as $z \in \mathbb{S}^*_{\text{VIX}'^2} \cap \mathbb{S}_w$ where $f_{\text{VIX}'^2}^{\text{2-SVCVJ++}}(z;\tau)$ is regular in the strip $\mathbb{S}_{\text{VIX}'^2}$ and $\mathbb{S}^*_{\text{VIX}'^2}$ is the conjugate strip, obtained via reflection with respect to the real z axis. The characteristic functions $f_{\text{VIX}'^2}^{\text{2-SVCVJ++}}(z;\tau)$ verifies

$$\left|f_{\text{VIX}'^2}^{\text{2-SVCVJ++}}(-z;\tau)\right| \ = \ \left|\mathrm{E}^{\mathbb{Q}}\left[e^{-iz\,\text{VIX}_T'^2}\,\middle|\,\mathcal{F}_t\right]\right| \ \le \ \mathrm{E}^{\mathbb{Q}}\left[\left|e^{-iz\,\text{VIX}_T'^2}\right|\,\middle|\,\mathcal{F}_t\right] \ = \ f_{\text{VIX}'^2}^{\text{2-SVCVJ++}}(-i\,\text{Im}(z);\tau) \tag{A.17}$$

and therefore, considering the relation in (A.14), determining the strip of regularity $\mathbb{S}^*_{\text{VIX}'^2}$ corresponds to analyze the stability of the solutions of the system ODEs in equation (A.2) for $z_k = -i\,\text{Im}(z)a_k(\bar{\tau})/\bar{\tau}$ and $k = 1, 2$. Similar arguments have been considered by (Lee, 2004; Andersen and Piterbarg, 2007; Lord and Kahl, 2010) in studying the regularity of the log-price characteristic function $f_x(z;\tau)$ of Heston-like stochastic volatility models. From the second of the (A.3), the solution $B_k^\sigma(-i\,\text{Im}(z)a_k(\bar{\tau})/\bar{\tau};\tau)$ is regular as long as its denominator is not equal to zero, requiring:

$$\text{Im}(z) < \zeta_c^{B_k^\sigma}(\tau) = \frac{\bar{\tau}}{a_k(\bar{\tau})}\frac{1}{\frac{\Lambda_k^2}{2\alpha_k}\left(1-e^{-\alpha_k\tau}\right)} \ , \tag{A.18}$$

which, in addition, guarantees the regularity of $A_k^\sigma(-i\,\text{Im}(z)a_k(\bar{\tau})/\bar{\tau};\tau)$, given in the first of (A.3). Idiosyncratic and correlated co-jumps solutions $C_{co}^\sigma(-i\,\text{Im}(z)a_1(\bar{\tau})/\bar{\tau};\tau)$ and $C_{id}^\sigma(-i\,\text{Im}(z)a_1(\bar{\tau})/\bar{\tau};\tau)$ are regular as long as the argument of the logarithms is not equal to zero, that requires, respectively:

$$\text{Im}(z) < \zeta_c^{C_{co}^\sigma}(\tau) = \frac{\bar{\tau}}{a_1(\bar{\tau})}\min\left(\frac{1}{\mu_{co,\sigma}}, \frac{1}{\frac{\Lambda_1^2}{2\alpha_1}\left(1-e^{-\alpha_1\tau}\right)+\mu_{co,\sigma}e^{-\alpha_1\tau}}\right) \ , \tag{A.19}$$

and

$$\text{Im}(z) < \zeta_c^{C_{id}^\sigma}(\tau) = \frac{\bar{\tau}}{a_1(\bar{\tau})}\min\left(\frac{1}{\mu_{id,\sigma}}, \frac{1}{\frac{\Lambda_1^2}{2\alpha_1}\left(1-e^{-\alpha_1\tau}\right)+\mu_{id,\sigma}e^{-\alpha_1\tau}}\right) \ . \tag{A.20}$$

We notice that, since $\mu_{co,\sigma}, \mu_{id,\sigma} > 0$, we have that $\min\left(\zeta_c^{C_{co}^\sigma}(\tau), \zeta_c^{C_{id}^\sigma}(\tau)\right) < \zeta_c^{B_1^\sigma}(\tau)$, and therefore $\zeta_c(\tau)$ is given by

$$\zeta_c(\tau) = \min\left(\zeta_c^{C_{co}^\sigma}(\tau), \zeta_c^{C_{id}^\sigma}(\tau), \zeta_c^{B_2^\sigma}(\tau)\right) \ . \tag{A.21}$$

Unreported results analyze the effect of the choice of the upper bound $\zeta_c(\tau)$ on the integrand behavior and pricing performance. Preliminary results show that the choice of $\text{Im}(z)$ does have an effect on the shape of the integrand (e.g. it corresponds to different values at $\text{Re}(z) = 0$), and on pricing results. For typical parameter values, as those shown in Table 4, we observe greater impact (roughly of order 10^{-4}) on VIX futures prices and on lower strikes and short-term options. The effect seems to be quite stable when the magnitude of the displacement ranges in typical values of order $I_\phi \approx 10^{-4}, 10^{-3}$. In the empirical analysis we use $\text{Im}(z) = \zeta_c(\tau)/2$. □

Proposition 4. *Under the $\mathcal{H}$++ models, the time t conditional central n-th moment*

$$k_{\text{VIX}}^{\mathcal{H}++}(n,t,T) = \mathrm{E}^{\mathbb{Q}}\left[\left(\text{VIX}_T - \mu_{t,T}^{\mathcal{H}++}\right)^n \,\middle|\, \mathcal{F}_t\right] \tag{A.22}$$

of the risk-neutral distribution of the forward VIX_T *is given by*

$$k_{\text{VIX}}^{\mathcal{H}++}(n,t,T) = \frac{1}{\pi}\int_0^{\infty} \text{Re}\left[f_{\sigma}^{\mathcal{H}}\left(-z\frac{a_1(\bar{\tau})}{\bar{\tau}}, -z\frac{a_2(\bar{\tau})}{\bar{\tau}}\right) e^{-iz\left(\sum_{k=1,2} b_k(\bar{\tau}) + I_{\phi}(T,T+\bar{\tau})\right)/\bar{\tau}} \hat{w}_n^{\mathcal{H}++}(z,t,T)\right] d\,\text{Im}(z) \ , \tag{A.23}$$

where $z = \text{Re}(z) + i\,\text{Im}(z) \in \mathbb{C}$, $0 < \text{Im}(z) < \zeta_c(\tau)$, *$\zeta_c(\tau)$ is given in equation (A.21),* $\mu_T^{\mathcal{H}++}$ *is the corresponding VIX Futures quotation*

$$\mu_{t,T}^{\mathcal{H}++} = \mathrm{E}^{\mathbb{Q}}\left[\,\text{VIX}_T \mid \mathcal{F}_t\right] \equiv F_{\text{VIX}}^{\mathcal{H}++}(t,T) \tag{A.24}$$

of Proposition 3 and the payoff transform $\hat{w}_n^{\mathcal{H}++}(z)$ *is known in closed form. Moreover, for* $n = 2,3,4$ *these are given by*

$$\begin{aligned}
\frac{\hat{w}_2^{\mathcal{H}++}(z,t,T)}{100^2} &= \frac{-1 + iz\mu^2 + \mu\sqrt{\pi}\sqrt{-iz}}{z^2} \ , \\
\frac{\hat{w}_3^{\mathcal{H}++}(z,t,T)}{100^3} &= \frac{3\sqrt{\pi} - 6iz\mu^2\sqrt{\pi} + (4iz\mu^3 - 12\mu)\sqrt{-iz}}{4(-iz)^{5/2}} \ , \\
\frac{\hat{w}_4^{\mathcal{H}++}(z,t,T)}{100^4} &= \frac{-2i - 6z\mu^2 + iz^2\mu^4 + \sqrt{\pi}(2z\mu^3 + 3i\mu)\sqrt{-iz}}{z^3} \ ,
\end{aligned} \tag{A.25}$$

respectively ($\mu = \mu_{t,T}^{\mathcal{H}++}/100$), which are single-valued regular functions provided that $\text{Im}(z) > 0$.

Proof of Proposition 4. Rewrite the kernel $\left(\text{VIX}_T - \mu_{t,T}^{\mathcal{H}++}\right)^n$ of the central moments $k_{\text{VIX}}^{\mathcal{H}++}(n,t,T)$ in (A.22) as non-linear functions, named $w_n^{\mathcal{H}++}$, of the squared index $\text{VIX}_t'^2 = (\text{VIX}_t/100)^2$

$$\frac{w_n^{\mathcal{H}++}(\text{VIX}_T'^2,t,T)}{100^n} = \left(\sqrt{\text{VIX}_T'^2} - \mu'\right)^n \ , \tag{A.26}$$

where $\mu = \mu_{t,T}^{\mathcal{H}++}/100$. Complex Fourier transforms $\hat{w}_n^{\mathcal{H}++}(z,t,T)$ of these functions are given by the integral

$$\frac{\hat{w}_n^{\mathcal{H}++}(z,t,T)}{100^n} = \int_0^{+\infty} e^{izx}\frac{w_n^{\mathcal{H}++}(x,t,T)}{100^n}dx \ , \tag{A.27}$$

that can be solved explicitly. Their expressions for $n = 2,3,4$ are shown in equations (A.25). Transforms $\hat{w}_n^{\mathcal{H}++}(z,t,T)$ are single-valued regular function in the upper half of the complex plane $z \in \mathbb{S}_w$ (A.13), that is $\text{Im}(z) > 0$. We can, therefore, follow the approach of Lewis (2000, 2001) stating the following:

$$\begin{aligned}
k_{\text{VIX}}^{\mathcal{H}++}(n,t,T) &= \mathrm{E}^{\mathbb{Q}}\left[\left(\text{VIX}_T - \mu_{t,T}^{\mathcal{H}++}\right)^n \,\middle|\, \mathcal{F}_t\right] = \mathrm{E}^{\mathbb{Q}}\left[w_n^{\mathcal{H}++}(\text{VIX}_T'^2,t,T) \,\middle|\, \mathcal{F}_t\right] \\
&= \mathrm{E}^{\mathbb{Q}}\left[\frac{1}{2\pi}\int_{i\,\text{Im}(z)-\infty}^{i\,\text{Im}(z)+\infty} e^{-iz\,\text{VIX}_T'^2}\hat{w}_n^{\mathcal{H}++}(z,t,T)dz \,\middle|\, \mathcal{F}_t\right] \\
&= \frac{1}{2\pi}\int_{i\,\text{Im}(z)-\infty}^{i\,\text{Im}(z)+\infty} \mathrm{E}^{\mathbb{Q}}\left[e^{-iz\,\text{VIX}_T'^2} \,\middle|\, \mathcal{F}_t\right]\hat{w}_n^{\mathcal{H}++}(z,t,T)dz \\
&= \frac{1}{2\pi}\int_{i\,\text{Im}(z)-\infty}^{i\,\text{Im}(z)+\infty} f_{\text{VIX}'^2}^{\mathcal{H}++}(-z;\tau)\hat{w}_n^{\mathcal{H}++}(z,t,T)dz \\
&= \frac{1}{2\pi}\int_{i\,\text{Im}(z)-\infty}^{i\,\text{Im}(z)+\infty} f_{\sigma}^{\mathcal{H}}\left(-z\frac{a_1(\bar{\tau})}{\bar{\tau}}, -z\frac{a_2(\bar{\tau})}{\bar{\tau}}\right) e^{-iz\left(\sum_{k=1,2} b_k(\bar{\tau}) + I_{\phi}(T,T+\bar{\tau})\right)/\bar{\tau}}\hat{w}_n^{\mathcal{H}++}(z,t,T)dz \ ,
\end{aligned} \tag{A.28}$$

from which the statement in Proposition 4 follows provided that $z \in \mathbb{S}^*_{\text{VIX}'^2} \cap \mathbb{S}_w$, that is $0 < \text{Im}(z) < \zeta_c(\tau)$, where $\zeta_c(\tau)$ is given in equation (A.21).

□

Appendix B. Calibration procedure

Appendix B.1. In sample calibration

We describe here the calibration procedure performed on each day t in sample. $\mathcal{H}$++ models depend on the set of affine parameters reported in Table 4, that we denote here synthetically as θ_t, and on the displacement function ϕ_t. On date t, joint calibration on the three markets is performed with Matlab's function `lsqnonlin` minimizing the loss function in (12), which we report again here highlighting the functional dependencies w.r.t. affine and displacement parameters

$$\begin{aligned} L(\theta_t, \phi_t) = &\frac{1}{N_{\text{SPX}}} \sum_{i=1}^{N_{\text{SPX}}} \left(\frac{\text{IV}^{\text{MKT}}_{i,\text{SPX}} - \text{IV}^{\text{mdl}}_{i,\text{SPX}}(\theta_t, \phi_t)}{\text{IV}^{\text{MKT}}_{i,\text{SPX}}} \right)^2 + \frac{1}{N_{\text{Fut}}} \sum_{j=1}^{N_{\text{Fut}}} \left(\frac{F^{\text{MKT}}_j - F^{\text{mdl}}_j(\theta_t, \phi_t)}{F^{\text{MKT}}_j} \right)^2 \\ &+ \frac{1}{N_{\text{VIX}}} \sum_{k=1}^{N_{\text{VIX}}} \left(\frac{\text{IV}^{\text{MKT}}_{k,\text{VIX}} - \text{IV}^{\text{mdl}}_{k,\text{VIX}}(\theta_t, \phi_t)}{\text{IV}^{\text{MKT}}_{k,\text{VIX}}} \right)^2 . \end{aligned} \tag{B.1}$$

The calibration of affine parameters θ_t simply requires positivity constraints on volatility factors' drift α_i, β_i, vol-of-vol Λ_i parameters, jumps intensities λ, λ', exponential jumps mean sizes $\mu_{co,\sigma}, \mu_{id,\sigma}$ and on the normal jumps dispersion parameter δ_x^2.

For what concerns the calibration procedure of the displacement ϕ_t, we provide a practical example and consider the market observed on the date t = Wednesday September 2nd 2009, which is shown in Figure 1.

Let us denote with T^t_{SPX} (respectively T^t_{VIX}) the set of maturities of SPX vanilla (resp. VIX derivatives) observed on date t and let $\tau^t_{\text{SPX}} = T^t_{\text{SPX}} - t$ (resp. $\tau^t_{\text{VIX}} = T^t_{\text{VIX}} - t$) the corresponding times to expiration. From Figure 1, we have

$$\tau^t_{\text{SPX}} = \{17, 28, ..., 290\} \text{ and } \tau^t_{\text{VIX}} = \{14, 49, 77, 105, ..., 196\} \tag{B.2}$$

days to maturity, with 105 days being the longest horizon at which VIX options are quoted in this date. From the results of Propositions 1 and 3, SPX vanilla and VIX derivatives prices depend on integrals of the form $I_\phi(t, T^t_{\text{SPX}})$ and $I_\phi(T^t_{\text{VIX}}, T^t_{\text{VIX}} + \bar{\tau}))$, which are equivalent to

$$\begin{aligned} I_\phi(t, T^t_{\text{SPX}}) = I_\phi(0, \tau^t_{\text{SPX}}) &= \int_0^{\tau^t_{\text{SPX}}} \phi_s ds \ , \\ I_\phi(T^t_{\text{VIX}}, T^t_{\text{VIX}} + \bar{\tau}) = I_\phi(\tau^t_{\text{VIX}}, \tau^t_{\text{VIX}} + \bar{\tau}) &= \int_{\tau^t_{\text{VIX}}}^{\tau^t_{\text{VIX}} + \bar{\tau}} \phi_s ds \ . \end{aligned} \tag{B.3}$$

The model constraint $\phi_t \geq 0$ translates into the constraints on the displacement's integrals

$$I_\phi(t, t + \tau) \geq 0 \ , \tag{B.4}$$

$\forall t, \tau \geq 0$, which we impose in the calibration procedure. Let us denote with $T^t = \{0 \cup T^t_{\text{SPX}} \cup T^t_{\text{VIX}} \cup T^t_{\text{VIX}} + \bar{\tau}\}$ the set of the relevant maturities (as included the set of the 30-days forward shifted maturities $T^t_{\text{VIX}} + \bar{\tau}$) in t and accordingly

$$\tau^t = T^t - t = \{0 \cup \tau^t_{\text{SPX}} \cup \tau^t_{\text{VIX}} \cup \tau^t_{\text{VIX}} + \bar{\tau}\} \tag{B.5}$$

the set of the relevant horizons. Time units have to be consistent, so if, as we have defined, $\bar{\tau} = 30/365$ years, then also τ^t_{SPX} and τ^t_{VIX} have to be measured in years. Horizons which are common to the different markets are counted just once. In our example: $N = 1 + 7 + 7 + 7$ (including the 0 at the beginning), because both SPX options and VIX futures have 7 horizons and $\tau^t_{\text{VIX}} + \bar{\tau}$ brings 7 more non-duplicated horizons. Therefore, in this case $\tau^t_N = \tau^t_{22} = 290$ days, coinciding with the last SPX options horizon, as it is usually found, being the SPX vanilla the longest quoted options.

At each Wednesday t in sample, the relevant integrals of ϕ_t are calibrated as follows:

1. Sort in ascending order all the N time to maturities $\tau^t_i \in \tau^t$ observed in the three markets in date t. Therefore, $\tau^t_1 = 0$ and τ^t_N is the longest horizon in τ^t.

2. Define the interval integrals

$$\Delta\Phi_i = I_\phi(\tau^t_i, \tau^t_{i+1}) = I_\phi(0, \tau^t_{i+1}) - I_\phi(0, \tau^t_i) \tag{B.6}$$

   $i = 1, ..., N-1$ and input them to the optimizer, imposing the positivity constraints $\Delta\Phi_i \geq 0$.

3. In the pricing routines, reconstruct the needed integrals of displacement as follows:

   (a) A SPX vanilla of k-th ranked horizon $\tau^t_k \in \tau^t_{\text{SPX}}$ can be constructed as:

$$I_\phi(\tau^t_1 = 0, \tau^t_k) = \sum_{i=1}^{k-1} \Delta\Phi_i \ . \tag{B.7}$$

   (b) A futures or option on VIX of p-th ranked horizon $\tau^t_p \in \tau^t_{\text{VIX}}$ and q-th ranked forward horizon $\tau^t_q \in \tau^t_{\text{VIX}} + \bar{\tau}$, with $q \geq p + 1$, can be constructed as:

$$I_\phi(\tau^t_p, \tau^t_q) = \sum_{i=p}^{q-1} \Delta\Phi_i \ . \tag{B.8}$$

The output of this calibration procedure is an optimal term structure of interval integrals at date t

$$\Delta\Phi^* = \{I^*_\phi(\tau^t_1 = 0, \tau^t_2), ..., I^*_\phi(\tau^t_{N-1}, \tau^t_N)\} \tag{B.9}$$

which is, by construction, consistent with the positive displacement constraint (B.4) and consistent with any functional form of the displacement ϕ_t having the same calibrated integrals (e.g. piecewise constant, piecewise linear, splines or other interpolation or functional methods). From the optimal interval integral term structure $\Delta\Phi^*$, the optimal displacement term structure $I^*_\phi(0, \tau^t)$ according to the market of date t can be reconstructed as the vector of

$$I^*_\phi(0, \tau^t_n) = \sum_{i=1}^{n-1} \Delta\Phi^*_i \tag{B.10}$$

$n = 2, ..., N$. In our example, the resulting calibrated displacement term structure (B.10) is shown in Figure B.9.

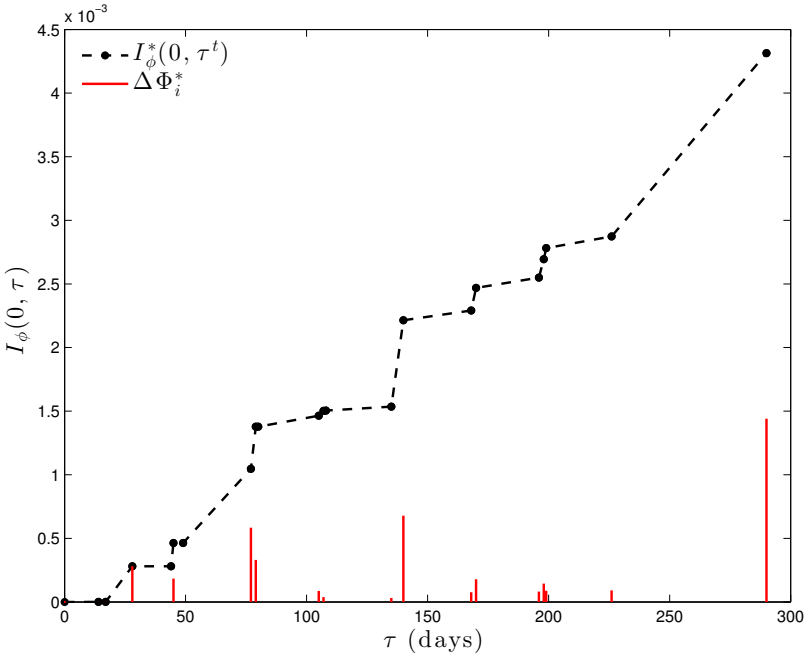

Figure B.9: This figure shows the optimal displacement term structure $I^*_\phi(0,\tau^t)$ of the 2-SVCVJ++ model calibrated on the three derivative markets observed on Wednesday September 2nd 2009, as reported in Figure (1). Black dots are calibrated $I^*_\phi(0,\tau^t_n)$ integrals for $\tau^t_1 = 0, \tau^t_2 = 14, ..., \tau^t_{22} = 290$ days to maturity. Red bars report the calibrated interval integrals $\Delta\Phi^*_i = I^*_\phi(\tau^t_i, \tau^t_{i+1})$, placed at the right edges τ^t_{i+1}, which are the (positively constrained) optimization variables.

Appendix B.2. Out of sample displacement interpolation

Let us denote with T^{t+n}_{SPX} and T^{t+n}_{VIX} the set of SPX and VIX markets maturities observed at date $t+n$. According to Propositions 1 and 3, to price out of sample SPX vanilla options (respectively VIX derivatives), we have to evaluate integrals like $I_\phi(t+n, T^{t+n}_{\text{SPX}})$ (resp. $I_\phi(T^{t+n}_{\text{VIX}}, T^{t+n}_{\text{VIX}} + \bar\tau)$).

Along the lines of the in-sample calibration above, we denote with $T^{t+n} = \{0 \cup T^{t+n}_{\text{SPX}} \cup T^{t+n}_{\text{VIX}} \cup T^{t+n}_{\text{VIX}} + \bar\tau\}$ the set of the relevant maturities observed in $t+n$, let $\tau^{t+n}_{\text{SPX}}(n) = T^{t+n}_{\text{SPX}} - (t+n)$ (resp. $\tau^{t+n}_{\text{VIX}}(n) = T^{t+n}_{\text{VIX}} - (t+n)$) represent the corresponding times to maturity - as computed from date $t+n$ - and define accordingly the set of relevant horizons

$$\tau^{t+n}(n) = T^{t+n} - (t+n) = \{0 \cup \tau^{t+n}_{\text{SPX}}(n) \cup \tau^{t+n}_{\text{VIX}}(n) \cup \tau^{t+n}_{\text{VIX}}(n) + \bar\tau\} \ . \tag{B.11}$$

To implement the out of sample pricing we have to evaluate the displacement term structure at date $t+n$:

$$I_\phi(t+n, T^{t+n}) = I_\phi(0, \tau^{t+n}(n)) = \int_0^{\tau^{t+n}(n)} \phi_s ds \ . \tag{B.12}$$

Moreover, for any $\hat\tau^{t+n}(n) = \hat T^{t+n} - (t+n) \in \tau^{t+n}(n)$ we have $I_\phi(t+n, \hat T^{t+n}) = I_\phi(0, \hat\tau^{t+n}(n))$, and

$$\begin{aligned} I_\phi(t+n, \hat T^{t+n}) &= I_\phi(t, \hat T^{t+n}) - I_\phi(t, t+n) \\ &= I_\phi(0, \hat\tau^{t+n}(0)) - I_\phi(0, n) \ , \end{aligned} \tag{B.13}$$

where $\hat\tau^{t+n}(0) = \hat T^{t+n} - t$ is the time-to-maturity of the contract expiring in date $\hat T^{t+n}$, as it was at date t, i.e. n days before. This allows to derive the integral $I_\phi(t+n, \hat T^{t+n})$ interpolating (and/or extrapolating) the

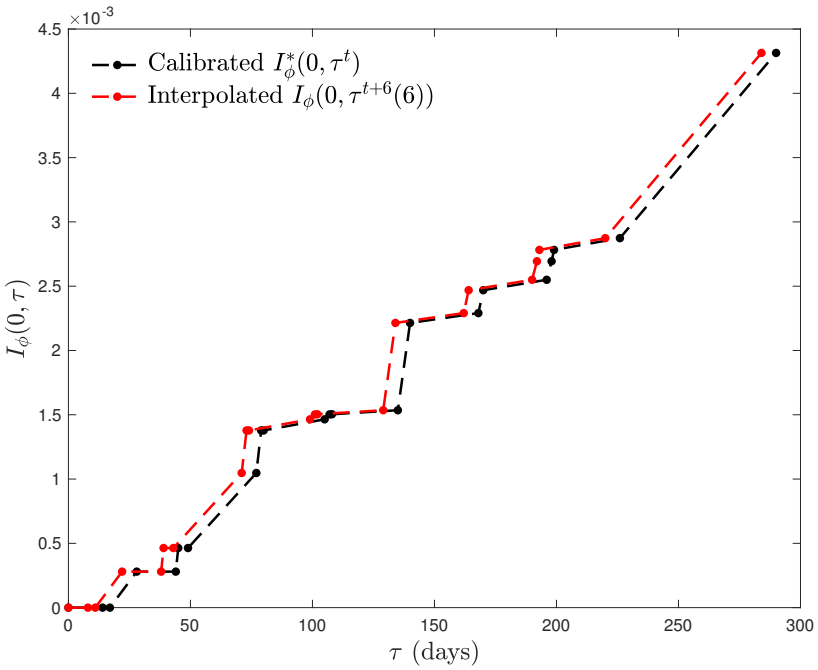

Figure B.10: This figure shows an example of out of sample displacement term structure. The term structure $I^*_\phi(0,\tau^t)$ in black, also reported in Figure (B.9) is calibrated on date t Wednesday September 2nd 2009 and is plotted at the horizons $\tau^t = T^t - t$. $I_\phi(0,\tau^{t+6}(6))$, in red, is derived from $I^*_\phi(0,\tau^t)$ according to equation (B.13) using a linear interpolation and is plotted at the horizons $\tau^{t+6}(6) = T^{t+6} - (t+6)$ observed on date $t+6$ Tuesday September 8th 2009.

calibrated term structure $I^*_\phi(0,\tau^t)$ in (B.10) at the horizons $\hat{\tau}^{t+n}(0)$ and for n days. As a minimal assumption in the out of sample pricing exercise of Section 4, we have opted for a linear interpolation.

Resuming the example considered in the previous section, we show, in Figure B.10 the derived term structure $I_\phi(0,\tau^{t+6}(6))$, in red, considered in the out of sample pricing on date $t+6$ (Tuesday, September 8th 2009), i.e. $n = 6$ days after the calibration date t (Wednesday, September 2nd 2009). Since, in this example, the contracts quoted in the out of sample date $t+6$ are exactly the same contracts quoted in t (that is, $T^{t+6} \equiv T^t$), the $I_\phi(0,\tau^{t+6}(6))$ term structure results in a rigid shift of $n = 6$ days towards shorter horizons of the calibrated term structure $I^*_\phi(0,\tau^t)$, according just to the aging $\tau^{t+6}(6) \equiv \tau^t - 6$ of the contracts.

References

Aït-Sahalia, Y., Lo, A. W., 1998. Nonparametric estimation of state-price densities implicit in financial asset prices. The Journal of Finance 53 (2), 499–547.

Amengual, D., Xiu, D., 2018. Resolution of policy uncertainty and sudden declines in volatility. Journal of Econometrics 203 (2), 297–315.

Andersen, L. B., Piterbarg, V. V., 2007. Moment explosions in stochastic volatility models. Finance and Stochastics 11 (1), 29–50.

Bakshi, G., Cao, C., Chen, Z., 1997. Empirical performance of alternative option pricing models. Journal of Finance 52, 2003–2049.

Bakshi, G., Kapadia, N., Madan, D., 2003. Stock return characteristics, skew laws, and the differential pricing of individual equity options. The Review of Financial Studies 16 (1), 101–143.

Bandi, F., Renò, R., 2016. Price and volatility co-jumps. Journal of Financial Economics 119, 107–146.

Bardgett, C., Gourier, E., Leippold, M., 2018. The information content of S&P 500 and VIX derivatives markets. Journal of Financial Economics, Forthcoming.

Bates, D., 1996. Jumps and stochastic volatility: Exchange rate processes implicit in deutsche mark options. Review of financial studies 9 (1), 69–107.

Bates, D., 2000. Post-'87 crash fears in the S&P 500 futures option market. Journal of Econometrics 94, 181–238.
Bayer, C., Gatheral, J., Karlsmark, M., 2013. Fast Ninomiya–Victoir calibration of the double-mean-reverting model. Quantitative Finance 13 (11), 1813–1829.
Bekaert, G., Engstrom, E., 2017. Asset return dynamics under habits and bad environment–good environment fundamentals. Journal of Political Economy 125 (3), 713–760.
Bekaert, G., Hoerova, M., 2014. The VIX, the variance premium and stock market volatility. Journal of Econometrics 183 (2), 181–192.
Black, F., 1976. The pricing of commodity contracts. Journal of Financial Economics 3, 167–179.
Black, F., Scholes, M., 1973. The pricing of options and corporate liabilities. Journal of Political Economy 81, 637–659.
Branger, N., Kraftschik, A., Völkert, C., 2014. The fine structure of variance: Consistent pricing of VIX derivatives in consistent and log-VIX models, working paper.
Brigo, D., Mercurio, F., 2001. A deterministic-shift extension of analytically-tractable and time-homogenous short-rate models. Finance & Stochastics 5, 369–388.
Broadie, M., Chernov, M., Johannes, M., 2007. Model Specification and Risk Premia: Evidence from Futures Options. The Journal of Finance 62 (3), 1453–1490.
Caporin, M., Kolokolov, A., Renò, R., 2017. Systemic co-jumps. Journal of Financial Economics 126 (3), 563–591.
Chen, H., Joslin, S., 2012. Generalized transform analysis of affine processes and applications in finance. Review of Financial Studies 25 (7), 2225–2256.
Chen, K., Poon, S.-H., 2013. Consistent pricing and hedging volatility derivatives with two volatility surfaces, working paper.
Cheridito, P., Filipović, D., Kimmel, R. L., 2010. A note on the Dai-Singleton canonical representation of affine term structure models. Mathematical Finance 20 (3), 509–519.
Christoffersen, P., Heston, S., Jacobs, K., 2009. The shape and term structure of the index option smirk: Why multifactor stochastic volatility models work so well. Management Science 55 (12), 1914–1932.
Chung, S.-L., Tsai, W.-C., Wang, Y.-H., Weng, P.-S., 2011. The information content of the S&P 500 index and VIX options on the dynamics of the S&P 500 index. Journal of Futures Markets 31 (12), 1170–1201.
Collin-Dufresne, P., Goldstein, R. S., Jones, C. S., 2008. Identification of maximal affine term structure models. The Journal of Finance 63 (2), 743–795.
Cont, R., Kokholm, T., 2013. A consistent pricing model for index options and volatility derivatives. Mathematical Finance 23 (2), 248–274.
Dai, Q., Singleton, K., 2002. Expectation puzzles, time-varying risk premia, and affine models of the term structure. Journal of Financial Economics 63, 415–441.
Detemple, J., Osakwe, C., 2000. The valuation of volatility options. European Finance Review 4 (1), 21–50.
Duan, J.-C., Yeh, C.-Y., 2010. Jump and volatility risk premiums implied by VIX. Journal of Economic Dynamics and Control 34 (11), 2232–2244.
Duffie, D., Kan, R., 1996. A yield-factor model of interest rates. Mathematical Finance 6 (4), 379–406.
Duffie, D., Pan, J., Singleton, K., 2000. Transform analysis and asset pricing for affine jump-diffusions. Econometrica 68 (6), 1343–1376.
Eraker, B., 2004. Do Stock Prices and Volatility Jump? Reconciling Evidence from Spot and Option Prices. The Journal of Finance 59 (3), 1367–1404.
Eraker, B., Johannes, M., Polson, N., 2003. The impact of jumps in volatility and returns. Journal of Finance 58, 1269–1300.
Grünbichler, A., Longstaff, F. A., 1996. Valuing futures and options on volatility. Journal of Banking & Finance 20 (6), 985–1001.
Heston, S., 1993. A closed-form solution for options with stochastic volatility with applications to bond and currency options. Review of Financial Studies 6, 327–343.
Jiang, G., Tian, Y., 2005. The model-free implied volatility and its information content. Review of Financial Studies 18 (4), 1305–1342.
Kokholm, T., Stisen, M., 2015. Joint pricing of VIX and SPX options with stochastic volatility and jump models. The Journal of Risk Finance 16 (1), 27–48.
Lee, R., 2004. Option pricing by transform methods: extensions, unification and error control. Journal of Computational Finance 7 (3), 51–86.
Lewis, A. L., 2000. Option Valuation under Stochastic Volatility. Finance Press.
Lewis, A. L., 2001. A simple option formula for general jump-diffusion and other exponential Lévy processes, unpublished manuscript.
Lian, G.-H., Zhu, S.-P., 2013. Pricing VIX options with stochastic volatility and random jumps. Decisions in Economics and Finance 36 (1), 71–88.
Lin, Y.-N., 2007. Pricing VIX futures: Evidence from integrated physical and risk-neutral probability measures. Journal of Futures Markets 27 (12), 1175–1217.

Lin, Y.-N., Chang, C.-H., 2009. VIX option pricing. Journal of Futures Markets 29 (6), 523–543.
Lo, C.-L., Shih, P.-T., Wang, Y.-H., Yu, M.-T., 2013. Volatility model specification: Evidence from the pricing of VIX derivatives, working paper.
Lord, R., Kahl, C., 2010. Complex logarithms in Heston-like models. Mathematical Finance 20 (4), 671–694.
Mencía, J., Sentana, E., 2013. Valuation of VIX derivatives. Journal of Financial Economics 108 (2), 367–391.
Pacati, C., Pompa, G., Renò, R., 2015. It's time to relax (the Feller condition), working paper.
Pacati, C., Renò, R., Santilli, M., 2014. Heston model: shifting on the volatility surface. Risk (November), 54–59.
Papanicolaou, A., Sircar, R., 2014. A regime-switching Heston model for VIX and S&P 500 implied volatilities. Quantitative Finance 14 (10), 1811–1827.
Psychoyios, D., Dotsis, G., Markellos, R. N., 2010. A jump diffusion model for VIX volatility options and futures. Review of Quantitative Finance and Accounting 35 (3), 245–269.
Sepp, A., 2008a. Pricing options on realized variance in the Heston model with jumps in returns and volatility. Journal of Computational Finance 11 (4), 33–70.
Sepp, A., 2008b. VIX option pricing in a jump-diffusion model. Risk (April), 84–89.
Song, Z., Xiu, D., 2016. A tale of two option markets: State-price densities and volatility risk. Journal of Econometrics 190, 176–196.
Tian, Y., Zili, Z., Lee, G., Klebaner, F., Hamza, K., 2015. Calibrating and pricing with a stochastic-local volatility model. Journal of Derivatives 22 (3), 21–39.
Todorov, V., Tauchen, G., 2011. Volatility jumps. Journal of Business and Economic Statistics 29, 356–371.
Whaley, R. E., 1993. Derivatives on market volatility: Hedging tools long overdue. Journal of Derivatives 1 (1), 71–84.
Zhang, J. E., Shu, J., Brenner, M., 2010. The new market for volatility trading. Journal of Futures Markets 30 (9), 809–833.
Zhang, J. E., Zhu, Y., 2006. VIX futures. Journal of Futures Markets 26 (6), 521–531.
Zhu, S.-P., Lian, G.-H., 2012. An analytical formula for VIX futures and its applications. Journal of Futures Markets 32 (2), 166–190.